NEOPLASIA
www.neoplasia.com

Volume 13 Number 9 September 2011 pp. 864–873 **864**

NRF2 Mutation Confers Malignant Potential and Resistance to Chemoradiation Therapy in Advanced Esophageal Squamous Cancer[1]

Abstract

Esophageal squamous cancer (ESC) is one of the most aggressive tumors of the gastrointestinal tract. A combination of chemotherapy and radiation therapy (CRT) has improved the clinical outcome, but the molecular background determining the effectiveness of therapy remains unknown. NRF2 is a master transcriptional regulator of stress adaptation, and gain-of-function mutation of NRF2 in cancer confers resistance to stressors including anticancer therapy. Direct resequencing analysis revealed that *Nrf2* gain-of-function mutation occurred recurrently (18/82, 22%) in advanced ESC tumors and ESC cell lines (3/10). The presence of *Nrf2* mutation was associated with tumor recurrence and poor prognosis. Short hairpin RNA–mediated down-regulation of NRF2 in ESC cells that harbor only mutated *Nrf2* allele revealed that the mutant NRF2 conferred increased cell proliferation, attachment-independent survival, and resistance to 5-fluorouracil and γ-irradiation. Based on the *Nrf2* mutation status, gene expression signatures associated with *NRF2* mutation were extracted from ESC cell lines, and their potential utility for monitoring and prognosis was examined in a cohort of 33 pre-CRT cases of ESC. The molecular signatures of *NRF2* mutation were significantly predictive and prognostic for CRT response. In conclusion, recurrent *NRF2* mutation confers malignant potential and resistance to therapy in advanced ESC, resulting in a poorer outcome. Molecular signatures of *NRF2* mutation can be applied as predictive markers of response to CRT, and efficient inhibition of aberrant NRF2 activation could be a promising approach in combination with CRT.

Neoplasia (2011) 13, 864–873

Introduction

Esophageal cancer (EC) is the sixth most common cause of cancer death worldwide [1]. The 5-year survival rate of patients with EC is reportedly less than 20%, making it one of the most aggressive tumors of the gastrointestinal tract [2]. Epidemiologically, alcohol consumption, cigarette smoking, and a preference for hot beverages, as well as the presence of Barrett esophagus resulting from gastroesophageal reflux, have been reported as risk factors for EC [3,4], and more than

Address all correspondence to: Tatsuhiro Shibata, MD, PhD, Cancer Genomics Project, National Cancer Center Research Institute, 5-1-1, Tsukiji, Chuo-ku, Tokyo, 104-0045, Japan. E-mail: tashibat@ncc.go.jp

[1]This study was supported in part by a Grant-in-Aid for the Comprehensive 10-Year Strategy for Cancer Control, the Grant-in-Aid for Cancer Research (19-1) from the Ministry of Health, Labor and Welfare, Japan and Research Grant of the Princess Takamatsu Cancer Research Fund 08-24007. The authors declare no conflicts of interest.
[2]This article refers to supplementary materials, which are designated by Tables W1 to W3 and Figures W1 to W4 and are available online at www.neoplasia.com.
Received 23 May 2011; Revised 24 June 2011; Accepted 27 June 2011

DOI 10.1593/neo.11750

460,000 patients develop this cancer annually worldwide [1]. Esophageal squamous cancer (ESC) is the predominant type of EC, being prevalent in Africa and Eastern Asia including Japan [5].

Currently, only surgical resection can be regarded as a curative therapy for ESC, and adjuvant or neoadjuvant combination of chemotherapy with radiation therapy (CRT) has recently improved the clinical outcome [6–8]. However, responsiveness to CRT varies among patients, and the molecular backgrounds that determine therapeutic effectiveness remain largely unknown [6]. Therefore, the discovery of molecular markers for precise prediction of responsiveness to therapy is eagerly anticipated. It is also necessary to construct effective personalized therapeutic modalities based on the molecular characterization of ESC.

Oxidative stress has been shown to play important roles in the carcinogenesis and progression of many cancers including ESC [9–11]. In response to intrinsic (e.g., reactive oxygen species generated in mitochondria) and extrinsic (e.g., radiation) oxidative stresses, NEF2L2 (nuclear erythroid factor 2-like 2, or NRF2) functions as a master transcriptional regulator of cytoprotective genes [12]. Under physiological conditions, KEAP1, an E3 ubiquitin ligase, directly interacts with two amino-terminal motifs (DLG and ETGE) of NRF2 and negatively regulates its expression level through the proteasome [13]. Recently, it has been revealed that aberrant activation of the NRF2 pathway occurs frequently in cancer. We and other groups have reported that the *Keap1* gene is inactivated in a wide range of cancers [14–18]. Moreover, we have discovered that the *Nrf2* gene is a *bona fide* oncogene in lung and head/neck cancers [19]. In the present study, we discovered that *NRF2* mutation also occurs frequently in ESC and examined its clinical significance especially from the viewpoint of responsiveness to CRT.

Materials and Methods

Clinical Samples and DNA Extraction

All surgical specimens were obtained from patients who had been diagnosed and had undergone surgery at the National Cancer Center Hospital, Tokyo, Japan (pathologic diagnoses are presented in Table W1). Tumor cells and corresponding lymphocytes or noncancerous tissues were dissected under a microscope from methanol-fixed or formalin-fixed (*in situ* carcinoma) paraffin-embedded tissues, and the DNA was extracted. High-molecular-weight DNA was also extracted from cell lines using DNAeasy (QIAGEN, Hamburg, Germany). Clinical data, including therapeutic response and prognosis, were collected from the medical charts. The protocol for analysis of the clinical samples was approved by the institutional review board of the National Cancer Center.

Polymerase Chain Reaction and Sequence Analysis

We amplified all exons of the Nrf2 gene by polymerase chain reaction (PCR) using High-Fidelity Taq polymerase (Roche Diagnostic, Basel, Switzerland), as described [19]. The PCR products were then purified (QIAquick PCR Purification Kit; QIAGEN) and analyzed by sequencing (Big Dye Sequencing Kit; Applied Biosystems, Carlsbad, CA).

Biologic and Biochemical Experiments

Ten ESC cell lines (KYSE-30, -50, -70, -110, -140, -150, -170, -180, -220, and -270) were obtained from the Japanese Collection of Research Bioresources (http://cellbank.nibio.go.jp) and maintained in Dulbecco modified Eagle medium supplemented with 10% fetal bovine serum. Construction of the retroviral expression vector of short hairpin RNA (shRNA) was carried out as described previously [20]. The shRNA-targeted sequences were as follows: NRF2–shRNA-1, ACTTGCTCAATGTCCTGTTGC; NRF2–shRNA-2, AGTTGAGCTTCATTGAACTGC. The control vector contains nontargeting shRNA sequence. The entry vectors were recombined with pDEST-CL-SI-MSCVpuro by LR reactions (Invitrogen, Carlsbad, CA), in accordance with the manufacturer's instructions. After infection (multiplicity of infection > 1), cells were selected and maintained in the presence of 1 μg/ml puromycin. NRF2 small interfering RNA (siRNA) was previously described [19]. NRF2-dependent luciferase activity was measured as described [15]. Cell proliferation was measured using the 96-well plate format by bromodeoxyuridine incorporation (Cell Proliferation ELISA; Roche Diagnostic). For attachment-free culture, 1×10^6 cells were seeded in ultra low-attachment dish (Ultra Low Cluster Plate, Corning, NY). 5-Fluorouracil (5-FU) was purchased from WAKO (Tokyo). Irradiation of cells was performed using the ^{60}Co source in the Gammacell 220 Research Irradiator (MDS Nordion, Ontario, Canada). The intracellular level of reduced glutathione was measured by GSH-Glo Glutathione Assay (Promega, Madison, WI). Protein extraction and immunoblot analysis were performed as described previously [15]. Antibodies used in this study are listed in Table W1.

Gene Expression Profiling and Quantitative Reverse Transcription–PCR

Ten micrograms of total RNA from ESC cell lines was reverse-transcribed by MMLV-RT, and a Cy3-labeled complementary RNA probe was synthesized using T7 RNA polymerase and hybridized with a microarray covering the whole human genome (Whole Human Genome Oligo Microarray, G4112F; Agilent Technologies, Santa Clara, CA). After washing, the microarray was scanned by the DNA microarray scanner (Agilent Technologies). Data were analyzed using GeneSpring software (Agilent Technologies). Quantitative reverse transcription (RT)–PCR was performed in triplicate and evaluated using universal probes for each amplicon and the LightCycler system (Roche). Primers designed by ProbeFinder (Version 2.45; Roche) and used in this study are shown in Table W2. The relative expression of each gene was determined by comparison with that of glyceraldehyde-3-phosphate dehydrogenase (GADPH).

Statistics

Statistical analysis of clinicopathologic data was performed using the StatView software package. Gene Set Enrichment Analysis (GSEA) was performed as follows. First, a gene list sorted in descending order based on fold change differences in expression between *NRF2*-mutated and wild-type ESC cell lines was calculated. Second, preranked GSEA was applied for the gene list to the C2 curated gene sets (MSigDB ver. 2.5) with default parameters (http://www.broadinstitute.org/gsea/index.jsp). Finally, significant gene sets were extracted if the false discovery rate (FDR) was less than 25%. To evaluate the predictive power of gene expression signatures for CRT and prognosis, biopsy samples with clinical information were classified into two groups by K-means clustering (R cluster package) using gene expression signatures for each significant gene set of GSEA, and then survival analysis was applied to the classified samples. The survival analysis was performed using the Kaplan-Meier method, and log-rank test was used to evaluate disease-free survival. To determine whether the NRF2 target genes based on ChIP-seq (chromatin immunoprecipitation sequence) [21] were enriched in any gene sets, we calculated the *P* values using the hypergeometric distribution for each the C2 curated gene sets and estimated the FDR.

Because the NRF2 ChIP-seq data were measured using a mouse cell line, we then converted the mouse genes to human genes using NCBI HomoloGene to apply them as a human gene set C2. We used a 10% FDR cutoff for this enrichment study.

Results

NRF2 *Mutation in ESC*

To evaluate the prevalence of *NRF2* mutation in human cancer, we attempted resequencing analysis of the entire coding region of the *NRF2* gene in a cohort (320 samples in total) of epithelial and nonepithelial tumors (pathologic diagnoses are shown in Table W2). We detected six nonsynonymous somatic mutations in the ECs (6/32, 18.8%) and one nonsynonymous somatic mutation in cervical cancer (1/18, 5.6%) and malignant melanoma (1/22, 4.5%), respectively (Figure 1*A* and Table 1). We additionally analyzed 50 cases of ESC and identified a total of 18 somatic mutations (18/82, 22%; Table 1). These mutations exclusively affected amino acid residues within and surrounding the KEAP1 binding motif, as reported previously in lung cancers [19]. We then analyzed 10 ESC cell lines and found three *NRF2*-mutated ones (3/10; Figure 1*B* and Table 1), of which two (KYSE70 and KYSE180) harbored homozygous mutations. *NRF2*-mutated KYSE70 and KYSE110 cells were established from poorly differentiated ESC. No *KEAP1* mutation was detected in ESC cases (data not shown). We additionally analyzed 36 cases of intraepithelial (*in situ*) ESC and detected no *NRF2* mutation (0/36), suggesting that *NRF2* mutation occurs predominantly at the advanced stage of esophageal carcinogenesis.

Association of NRF2 *Mutation with Tumor Recurrence and Poor Prognosis of ESC*

To further determine the clinical significance of *NRF2* gene mutation in EC, we analyzed the association between *NRF2* mutation status and clinicopathologic factors. The presence of *NRF2* mutation was correlated with tumor recurrence ($P = .046$) and tended to be associated with lymph node metastasis ($P = .072$). Patients with *NRF2*-mutated tumors showed poorer survival ($P = .005$; Table 2 and Figure 1*C*). Clinical stage ($P = .038$) and lymph node metastasis ($P = .039$) were associated with the disease-free survival of the patient (Table 2).

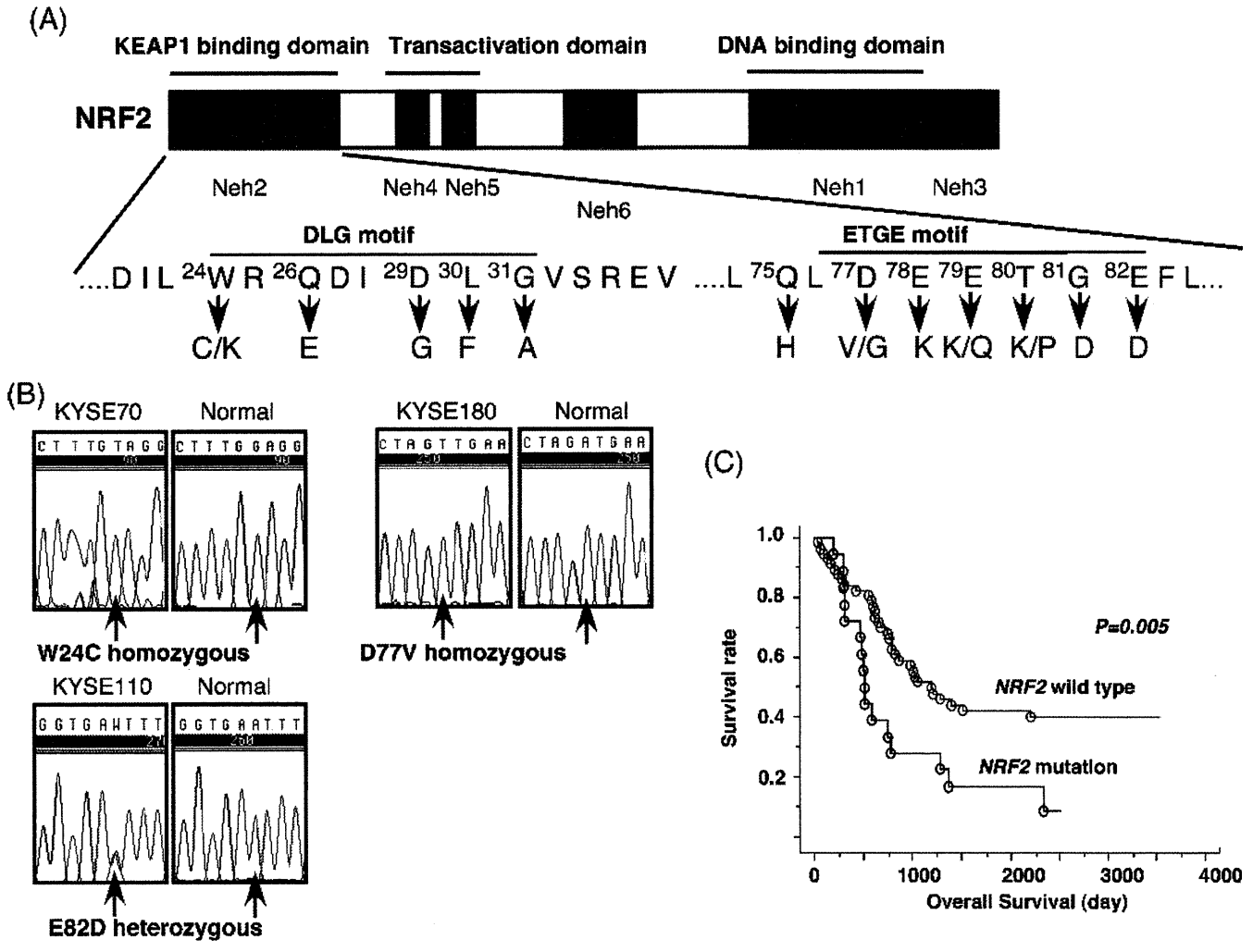

Figure 1. *NRF2* mutation in EC. (A) Somatic NRF2 mutations are clustered in the KEAP1 binding domain. Schematic presentation of NRF2 protein indicates the location of Neh1~6 (Nrf2-ech homology) domains and functional annotations. Somatic mutations identified in this study (blue) affected amino acids in the DLG or ETGE motifs. (B) Sequence chromatography of NRF2 mutations in ESC cell lines with corresponding normal sequences in the bottom panel. KYSE70 and KYSE180 cells harbor homozygous mutations. (C) Kaplan-Meier plot showing overall survival of ESC patients segregated according to NRF2 mutation status.

Table 1. *NRF2* Mutation in Human Cancers.

Sex	Tumor Type	Nucleotide Substitution	Amino Acid Change	Zygosity
M	Esophageal cancer (SCC)	c. 70T>C	p. W24K	Heterozygous
F	Esophageal cancer (SCC)	c. 72G>C	p. W24C	Heterozygous
M	Esophageal cancer (SCC)	c. 76C>G	p. Q26E	Heterozygous
M	Esophageal cancer (SCC)	c. 66A>G	p. D29G	Heterozygous
M	Esophageal cancer (SCC)	c. 66A>G	p. D29G	Allelic imbalance (mut > wt)
M	Esophageal cancer (SCC)	c. 88C>T	p. L30F	Heterozygous
M	Esophageal cancer (SCC)	c. 92G>C	p. G31A	Heterozygous
M	Esophageal cancer (SCC)	c. 225A>C	p. Q75H	Heterozygous
M	Esophageal cancer (SCC)	c. 230A>T	p. D77V	Heterozygous
M	Esophageal cancer (SCC)	c. 230A>G	p. D77G	Heterozygous
M	Esophageal cancer (SCC)	c. 232G>A	p. E78K	Heterozygous
M	Esophageal cancer (SCC)	c. 235G>A	p. E79K	Heterozygous
M	Esophageal cancer (SCC)	c. 235G>A	p. E79K	Heterozygous
M	Esophageal cancer (SCC)	c. 235G>A	p. E79K	Heterozygous
M	Esophageal cancer (SCC)	c. 235G>A	p. E79K	Heterozygous
M	Esophageal cancer (SCC)	c. 239C>A	p. T80K	Heterozygous
F	Esophageal cancer (SCC)	c. 238A>C	p. T80P	Heterozygous
F	Esophageal cancer (SCC)	c. 242G>A	p. G81D	Heterozygous
M	Malignant melanoma	c. 88C>T	p. L30F	Heterozygous
F	Cervical cancer (SCC)	c. 235G>C	p. E79Q	Heterozygous
M	KYSE70: Esophageal cancer (SCC)	c. 72G>T	p. W24C	Homozygous
M	KYSE110: Esophageal cancer (SCC)	c. 246A>T	p. E82D	Heterozygous
M	KYSE180: Esophageal cancer (SCC)	c. 230A>T	p. D77V	Homozygous

Mutant NRF2 Has a Gain-of-Function Activity and Regulates Proliferation and Attachment-Independent Cell Survival in ESC Cells

We compared the transcriptional activities of ESC-associated NRF2 mutants (W24C and D77V) to that of wild NRF2 and determined that mutant NRF2 has a gain-of-function activity, which is partly resistant to KEAP1-mediated inhibition (Figure 2*A*). There was no significant difference in transcriptional activity between homozygous (KYSE30) and heterozygous (KYSE110) mutant cells (Figure W1).

The previously mentioned analysis of clinical samples suggested that *NRF2* mutation plays a role in metastasis and tumor progression of ESC. Exploiting our discovery of ESC cell lines with homozygous *NRF2* mutation, we established KYSE70 cells stably expressing shRNAs against *NRF2* to examine the biologic features solely regulated by mutant NRF2. We tested two different lentiviruses containing NRF2-targeted shRNA (shRNA-1 and -2) along with a control virus. Immunoblot analysis revealed that NRF2–shRNA-2 robustly (11.4% of control) reduced the expression of endogenous mutant NRF2 protein compared with the NRF2–shRNA-1 clone (71.2% of control) (Figure 2*C*). Similarly, NRF2-dependent transcriptional activity markedly decreased (8.9% of control) in shRNA-2 clone (Figure 2*D*).

Table 2. Associations among *NRF2* Mutation Status, Clinicopathologic Factors, and Prognosis.

Clinicopathologic Factor		No. Patients	*NRF2* Mutation, *P*	Overall Survival, *P*	Disease-free Survival, *P*
Sex	Male	69	.914	.119	.656
	Female	13			
NRF2 mutation	+	18	na*	.005	.288
	–	64			
Smoking	+	64	.302	.572	.557
	–	18			
Alcohol intake	+	71	.268	.366	.143
	–	11			
Stage	I-II	25	.709	.895	.038
	III-IV	57			
Invasion depth	>a1	66	.186	.453	.565
	<mp	16			
Lymph node metastasis	+	65	.072	.285	.039
	–	17			
Histologic differentiation	Well	11	.134	.7	.074
	Mod	33			
	Poor	38			
Lymphatic infiltration	+	60	.48	.746	.336
	–	22			
Venous involvement	+	54	.631	.215	.124
	–	28			
Intramucosal metastasis	+	10	.873	.376	.654
	–	72			
Tumor recurrence	+	47	.046	.587	.775
	–	35			

"+" indicates positive; "–," negative; >a1, invade beyond muscularis propria; <mp invade within muscularis propria; well, well differentiated; mod, moderately differentiated; poor, poorly differentiated.
*Not applicable.

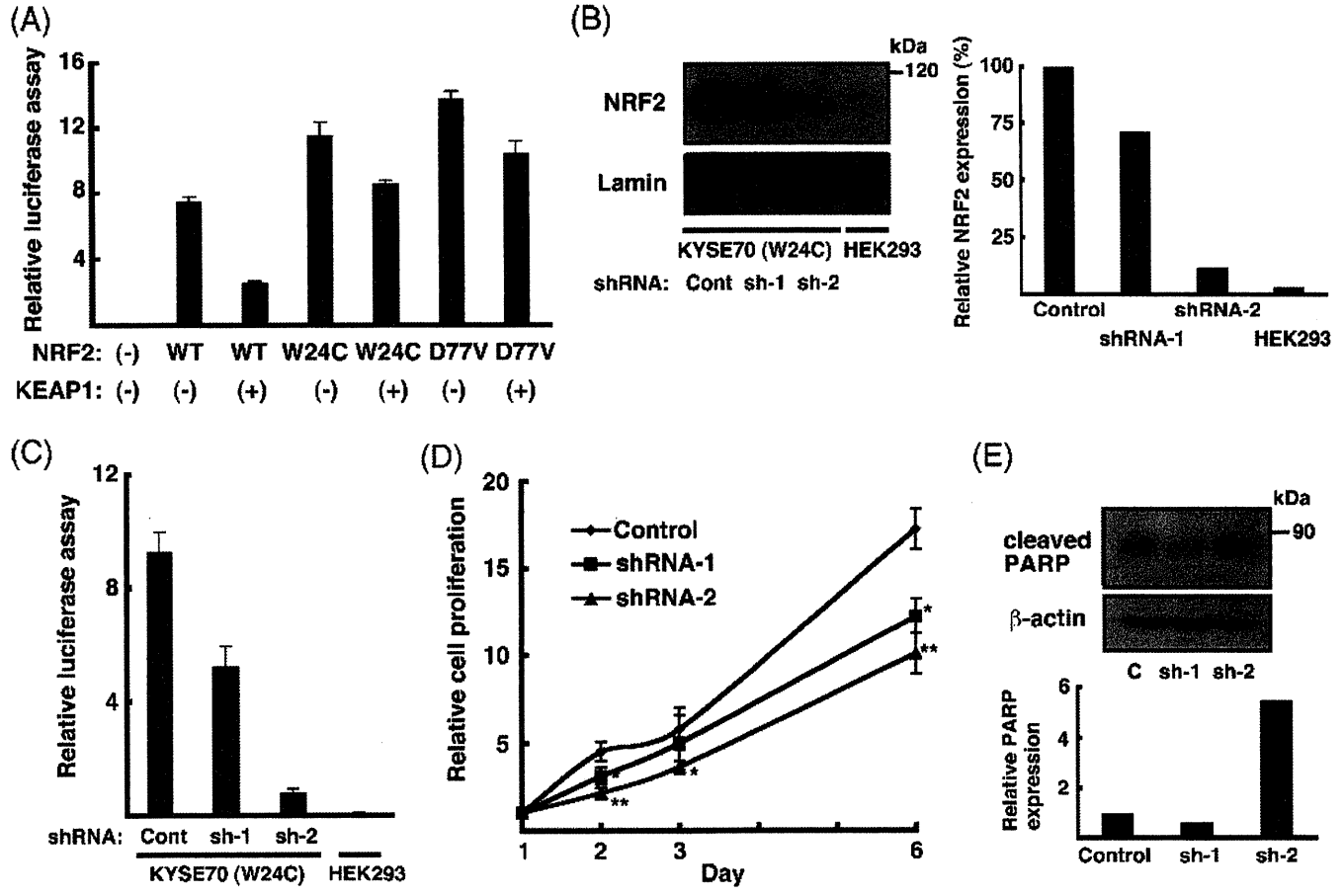

Figure 2. Down-regulation of gain-of-function NRF2 mutant in KYSE70 cells by shRNA. (A) Transcriptional activities of wild-type and ESC-associated mutant NRF2 were measures in the absence or presence of the *Keap1* gene. (B) Down-regulation of NRF2 protein in KYSE70 cells treated with NRF2-targeting shRNAs. Left, Immunoblot analysis of NRF2 protein in the nuclear fraction of KYSE70 cells infected with GFP shRNA (cont) or two different NRF2–shRNAs (sh-1 and sh-2). HEK293 cells lack NRF2 accumulation and were loaded as a negative control. Lamin B1 was used as a loading control. Right, Relative NRF2 expression in each clone was presented. (C) NRF2-dependent transcriptional activities of KYSE clones and HEK293. (D) Cell proliferation plot of KYSE70 clones infected with control or NRF2–shRNAs (shRNA-1 and shRNA-2). Data are mean ± SD of three independent experiments. $*P < .05$, $**P < .01$. (E) KYSE70 clones were cultured on an ultra low-attachment plate for 72 hours, and whole proteins were then extracted. Expression of cleaved PARP was examined by immunoblot analysis. β-Actin was used as a loading control. Relative PARP1 expression compared with the control shRNA was shown below. Molecular marker is indicated on the right (kDa).

Both shRNAs reduced cell proliferation in KYSE70 cells (Figures 2*E* and W2). We then measured attachment-independent cell survival in liquid culture, which mimics the antiapoptotic activity of floating cancer cells in tumor metastasis or recurrence. As shown in Figure 2*C*, only shRNA-2 clones exhibited more apoptosis in culture conditions where adhesion to a substrate was inhibited.

Down-regulation of Mutant NRF2 Increases the Sensitivity of ESC Cells to 5-FU

Previous studies have shown that activation of NRF2 in lung and gallbladder cancers confers resistance to chemotherapeutic drugs [14,15]. To determine whether NRF2 activation has any association with drug resistance in ESC cells, we examined the sensitivity to 5-FU, a commonly used chemotherapeutic reagent for ESC, in ESC cells. We found that NRF2-mutated cells were relatively resistant to 5-FU treatment compared with an NRF2 wild-type cell (Figure W3*A*) and that NRF2–downregulated KYSE70 cells (both shRNA-1 and shRNA-2 clones) showed increased sensitivity to 5-FU (the IC_{50} of each clone was 125.3, 81.3, and 13.1 μM respectively; Figure 3*A*). We also reduced the expression of NRF2 in other *NRF2*-mutated ESC cells using NRF2 siRNA and tested their sensitivity to 5-FU. This yielded results similar to that for KYSE70 cell (Figure 3*B*).

Robust Down-regulation of Mutant NRF2 Is Required for Enhancing Radiation Sensitivity in ESC Cells

Radiation therapy induces oxidative stress by producing reactive oxygen species in cancer cells. Thus, it is very likely that *NRF2* mutation is associated with radiosensitivity. To determine whether mutant NRF2 has a role in acquisition of resistance to irradiation, we exposed control and NRF2 shRNA-infected KYSE70 cells to γ-irradiation (2 Gy) and examined their clonogenic activities (basal colony formation activity of ESC cells is shown in Figure W3*B*), which reflect the degree of irradiation-induced cellular damage. As shown in Figure 3*C*, NRF2-downregulated cells (both shRNA-1 and shRNA-2 clones) were more sensitive to irradiation than control clone. However, when the relative number of colonies was compared among three clones, only the shRNA-2 clone showed a significant reduction ($P = .0002$). This suggests that moderate (~70%) NRF2

down-regulation affected the colony formation activity but that a more complete reduction (~10%) of mutant NRF2 would be required to enhance radiation sensitivity.

It has been reported that the intracellular glutathione level is correlated with sensitivity to radiation [22,23]. To determine whether mutant NRF2 has any role in regulating the level of glutathione in irradiated ESC cells, we measured the expression of major enzymes (glutamate-cysteine ligase, catalytic subunit [GCLC] and glutathione reductase [GSR]), which regulate glutathione synthesis and modification and are direct targets of NRF2 [21,24], in NRF2-downregulated KYSE70 cells exposed to various doses of irradiation. Quantitative RT-PCR analysis revealed that down-regulation of mutant NRF2 (shRNA-2 clone) was significantly reduced not only for the inducible expressions of GCLC and GSR but also for their basal level (Figure 3*D*). Interestingly, this reduction was not obvious in the shRNA-1 clone, which is consistent with the radiation sensitivity experiment previously mentioned and suggests that robust NRF2 down-regulation would be required for decreasing glutathione-regulatory enzymes (Figure 3*D*). Consistently, the basal level and radiation-induced increase of reduced glutathione were diminished only in the shRNA-2 clone (Figure W4).

Molecular Signatures Associated with NRF2 *Mutation Are Prognostic Factors for ESC and Predictive of Response to CRT*

These *in vitro* data strongly suggested that NRF2 activation by genetic alteration could be associated with the clinical response to CRT. However, the previously mentioned ESC cohort, whose *NRF2* mutation status was determined, contained only eight cases that had received postoperative CRT. Despite the difficulty in obtaining molecular data from minute biopsy samples of tumors before treatment, we

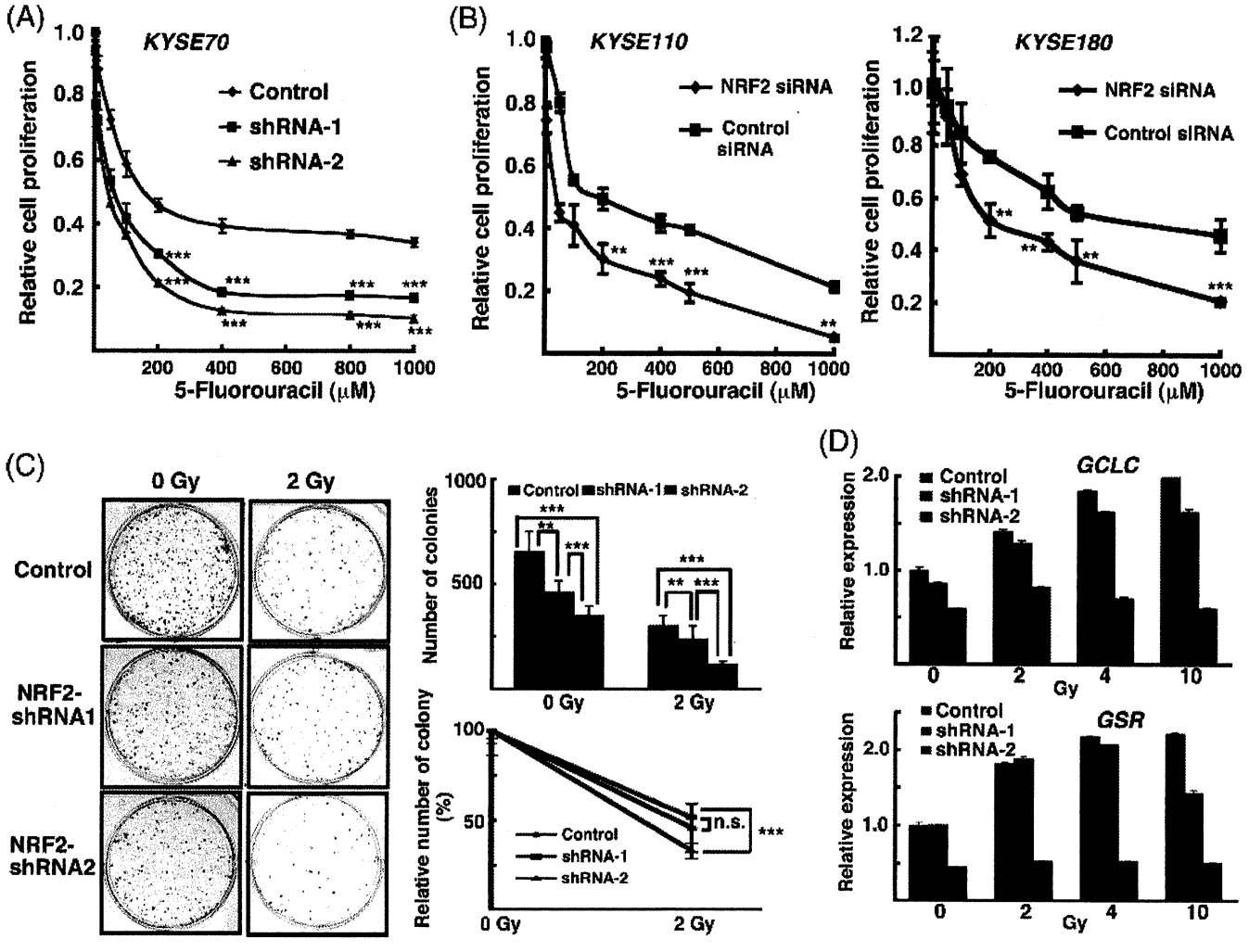

Figure 3. Mutant NRF2 confers resistance to chemotherapeutic reagent and radiation. (A) KYSE70 clones infected with control shRNA or NRF2–shRNAs were treated with various concentrations of 5-FU. (B) KYSE180 and KYSE110 cells were treated with control or NRF2 siRNA and various concentrations of 5-FU, as in A. Data represent cell viability after 48 hours relative to vehicle (DMSO)-treated control. Data are mean ± SD of three independent experiments; statistical difference to control siRNA or shRNA, $^{**}P < .01$, $^{***}P < .001$. (C) Left, A representative plate showing colony formation by each clone with control (0 Gy) and 2-Gy irradiation. Top right, Number of KYSE70 clones infected with control shRNA and NRF2–shRNAs that formed colonies after control (0 Gy) and 2-Gy irradiation. Data are mean ± SD of eight independent plates. Bottom right, The relative number of colonies after 2-Gy irradiation compared with the control (0 Gy). Note that the difference between control shRNA and shRNA-1 clones was not significant (n.s.). (D) KYSE70 clones were irradiated with different doses, and the expression of GCLC and GSR mRNAs was then examined. Data are mean ± SD of three independent experiments, $^{**}P < .01$. $^{***}P < .001$.

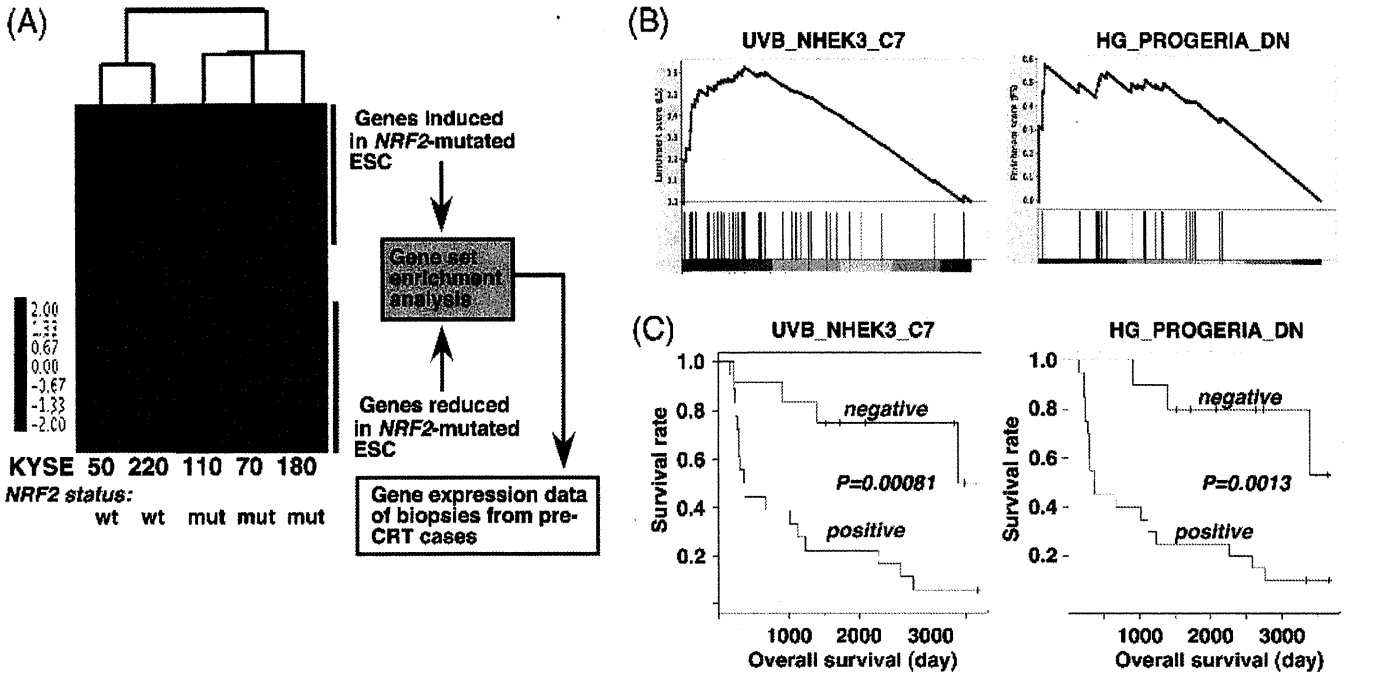

Figure 4. Pathway signatures of mutant NRF2 are associated with ESC patients' survival after CRT. (A) Two-dimensional hierarchal clustering of KYSE cells by genome-wide gene expression. NRF2 mutation status is shown at the bottom. GSEA extracted characteristic gene sets enriched in NRF2-mutated or wild-type ESC cells, and their prognostic significance was evaluated based on gene expression data for biopsies from pre-CRT cases. (B) Representative panels showing results of GSEA of genes enriched in NRF2-mutated ESC cell lines. (C) Kaplan-Meier plot showing overall survival of ESC patients after CRT segregated according to the NRF2 mutant signature.

previously collected the gene expression profiles of 33 pre-CRT samples of ESC for which the same therapeutic protocol had been used and for which the therapeutic response had been clinically evaluated [25]. Therefore, using this data set, we attempted to analyze whether the gene expression signatures associated with *NRF2* mutation could be predictive markers of response to CRT in ESC.

For this purpose, we first obtained the genome-wide gene expression data for five ESC cell lines and extracted the *NRF2*-mutated ESC signature based on the *NRF2* mutation status (Figure 4*A*). Using GSEA, we obtained a panel of molecular pathway signatures that were significantly associated with *NRF2* mutation status (representative pathways are shown in Figure 4*B*). The expressions of 703 gene sets were increased, and those of 14 gene sets were decreased in *NRF2*-mutated ESC cell lines (a complete list is shown in Table W3). We then tested whether changes in the expression of any of these signatures were associated with the clinical response to CRT and overall survival after treatment. We found that the increased expression of 15 gene sets was significantly ($P < .05$) associated with both poor response to CRT and a poor patient outcome after CRT (Table 3; representative Kaplan-Meier plots are shown in Figure 4*C*). All of the potentially predictive molecular signatures were increased in *NRF2*-mutated ESC cell lines and included pathways related to the oxidative stress response ($n = 4$), immune/cytokine response ($n = 4$), and hematopoietic disorder ($n = 3$) (Table 3). We further elucidated that direct NRF2 target genes confirmed by a combination of ChIP-seq and microarray analysis [21] were significantly

Table 3. Mutant NRF2 Signatures Associated with CRT Response.

Molecular Pathways	Prognosis, *P*	Clinical Response, *P*	NRF2 Target Enrichment, *P*	No. NRF2 Target Genes	Functional Annotation
ET743PT650_COLONCA_DN	.000103	.00404	.000917	7	Anticancer drug
GLYCOSPHINGOLIPID_METABOLISM	.000744	.00519	.585	1	Glycolipid metabolism
UVB_NHEK3_C7	.000813	.0235	.00279	7	Oxidative stress response
HG_PROGERIA_DN	.00132	.0109	.6	1	Aging
TAKEDA_NUP8_HOXA9_16D_UP	.00306	.0186	.318	8	Hematopoietic disorder
CARIES_PULP_HIGH_UP	.00466	.0186	.865	2	Immune/cytokine response
ABRAHAM_AL_VS_MM_UP	.0083	.00688	.254	2	Hematopoietic disorder
ABRAHAM_MM_VS_AL_DN	.0083	.00688	.24	2	Hematopoietic disorder
IFN_GAMMA_UP	.00847	.045	.165	3	Immune/cytokine response
AS3_FIBRO_C4	.00865	.0235	1	0	Oxidative stress response
TSADAC_RKOSILENT_UP	.0115	.045	.52	1	Methylated in colon cancer
BRCA1KO_MEF_DN	.0144	.0174	.0267	7	Oxidative stress response
UVB_SCC_DN	.016	.0235	.899	2	Oxidative stress response
CMV_HCMV_TIMECOURSE_24HRS_DN	.0196	.045	.0169	5	Immune/cytokine response
SANA_TNFA_ENDOTHELIAL_UP	.0286	.00669	.587	3	Immune/cytokine response

Table 4. NRF2 Target Genes Enriched in the CRT-predictive Pathways.

Pathway	Gene Symbol	Gene Name
ET743PT650_COLONCA_DN	*MGMT*	O^6-methylguanine-DNA methyltransferase
	LRBA	LPS-responsive vesicle trafficking, beach, and anchor containing
	KIFAP3	Kinesin-associated protein 3
	IRS1	Insulin receptor substrate 1
	GBE1	Glucan (1,4-alpha-), branching enzyme 1 (glycogen branching enzyme, Andersen disease, glycogen storage disease type IV)
	ADK	Adenosine kinase
	BRE	Brain and reproductive organ-expressed (TNFRSF1A modulator)
UVB_NHEK3_C7	*PGD*	Phosphogluconate dehydrogenase
	ESD	Esterase D/formylglutathione hydrolase
	ADK	Adenosine kinase
	PAM	Peptidylglycine alpha-amidating monooxygenase
	AKR1A1	Aldo-keto reductase family 1, member A1 (aldehyde reductase)
	CDKN3	Cyclin-dependent kinase inhibitor 3 (CDK2-associated dual-specificity phosphatase)
	PLA2G4A	Phospholipase A2, group IVA (cytosolic, calcium-dependent)
BRCA1KO_MEF_DN	*PDIA4*	Protein disulfide isomerase family A, member 4
	GPT2	Glutamic pyruvate transaminase (alanine aminotransferase) 2
	MAN1A1	Mannosidase, alpha, class 1A, member 1
	LAMC1	Laminin, gamma 1 (formerly LAMB2)
	ADD3	Adducin 3 (gamma)
	CDC2L6	Cell division cycle 2-like 6 (CDK8-like)
	KLF9	Kruppel-like factor 9
CMV_HCMV_TIMECOURSE_24HRS_DN	*WNT5A*	Wingless-type MMTV integration site family, member 5A
	SERPINE1	Serpin peptidase inhibitor, clade E (nexin, plasminogen activator inhibitor type 1), member 1
	ANXA1	Annexin A1
	VEGFC	Vascular endothelial growth factor C
	ADD3	Adducin 3 (gamma)

enriched in part of these pathways (Table 2; enriched genes are listed in Table 4).

Discussion

NRF2 *Mutation in ESC*

In the present study, we conducted mutation screening of the *Nrf2* gene in a wide range of tumor types including sarcoma and found that *NRF2* mutation is specifically frequent in EC and rarely occurs in cervical cancer and melanoma. These ESC-associated mutations harbor gain-of-function activity. Because *Keap1* recognizes two distinct regions of NRF2, single amino acid change may not completely inhibit *Keap1*-mediated degradation or sequestration [19]. Recently, Kim et al. [26] performed a mutation screening of hot spots in the *Nrf2* gene in more than 1000 tumors and reported that *NRF2* mutation is recurrent in tumors of the lung, skin, esophagus, and larynx, which is concordant with our previous and current observations. We previously reported that *NRF2* mutation was more common in smoking-associated lung cancer [19]; however, we failed to demonstrate any significant association between the presence of *NRF2* mutation and smoking history (P = .302) in ESC, probably because most of the affected patients in our cohort (64/82, 78%) were smokers. Also, *NRF2* mutation status was not associated with the habitual alcohol intake (P = .268). Previous genetic analyses have shown that polymorphisms of the *GSTP1* and *NQO1* genes, both of which are known direct targets of NRF2, are associated with susceptibility to ESC in Asian and white populations [27–29]. It would be interesting to examine the frequency of *NRF2* mutation in other ESC cohorts with different genetic, epidemiological, or ethnic backgrounds.

Because *Keap1*-deleted mice show hyperkeratosis in the forestomach [30], which is analogous to the esophagus, NRF2 activation could affect differentiation process of esophageal epithelium, which might be associated with malignant features of ESC. Our analysis of a cohort of ESC cases has further revealed the clinical significance of *NRF2* mutation. Our mutation analysis revealed that *NRF2* mutation was only detected in the late stage ESC. The presence of *NRF2* mutation was associated with tumor recurrence and was shown to be a significant prognostic factor. A recent study aimed at identifying NRF2 target genes by ChIP-seq has revealed that NRF2 directly regulates the expression of gene groups that are related to cell proliferation and survival, in addition to the detoxification response [21]. Using ESC cell lines containing *NRF2* mutation, we found that mutant NRF2 promotes ESC cell proliferation. We further revealed that mutant NRF2 confers attachment-independent cell survival, which is intimately associated with lymph node metastasis and tumor progression. Collectively, our results demonstrate that aberrant NRF2 activation resulting from its genetic alteration occurs at a relatively advanced stage of ESC and that it induces cell proliferation and survival signals, resulting in acquisition of malignant features and poor prognosis.

Molecular Signature of NRF2 *Mutation and Chemoradiation Therapy in ESC*

In addition to these malignant characters of cancer cells, resistance to current therapies would also be associated with a poorer survival rate. Previous studies have shown that NRF2 activation by loss-of-function mutations or down-regulation of the *Keap1* gene confers resistance to chemotherapeutic drugs and radiation [14,15,18,31]. As has been reported in lung cancer [19], down-regulation of mutant NRF2 enhanced the sensitivity of ESC cells to a chemotherapeutic agent. Furthermore, mutant NRF2 regulates resistance to irradiation partly through induction of enzymes related to glutathione synthesis. Consequently, effective inhibition of aberrant NRF2 signaling could offer a novel therapeutic approach for ESC in combination with CRT. Interestingly, robust reduction of mutant NRF2 was required to inhibit

resistance to radiation and induction of glutathione-regulating enzymes. Combined with other analyses, it could be possible that there are distinct groups of target genes regulated by mutant NRF2 in ESC cells. One group is sensitive to the amount of NRF2 and includes genes associated with cell proliferation, colony formation, and 5-FU resistance. The other is relatively resistant to NRF2 reduction and is responsible for attachment-independent survival and radiation resistance.

Our *in vitro* analyses also suggest that NRF2 activation could be associated with a poorer response to CRT in clinical cases of ESC. To examine this hypothesis, we carried out gene expression profiling, in view of the difficulty in collecting sufficient samples of pre-CRT tumors for mutation analysis. A number of previous studies have reported the identification of biomarkers that are predictive of the response of ESC to 5-FU or 5-FU–based neoadjuvant CRT [32–34]. Previously reported molecular makers have been categorized into several groups, including those related to 5-FU metabolism (e.g., thymidylate synthase and thymidine phosphorylase), the DNA repair pathway (e.g., excision repair cross-complementing rodent repair deficiency, complementation group 1 [ERCC1] and TP53), hypoxia (hypoxia-inducible factor 1α and vascular endothelial growth factor), and apoptosis/survival signaling (e.g., survivin, Bax, epidermal growth factor receptor, and Cox2) [32]. We tested the association between the expression level of ERCC1 or survivin and the clinical response to CRT in our cohort, but found no significant relationship (ERCC1, $P = .209$; survivin, $P = .327$). In contrast to these studies focusing on molecules with functional associations, only a few studies have explored microarray data in an unbiased way to search for biomarkers predictive of CRT efficacy, and only a limited number of cases ($n = 13$, 19, or 20) were examined [35–37].

In the present study, we adopted a different approach because NRF2 regulates a network of genes related to various molecular pathways at a different dose-response interaction. Instead of focusing on the expression of individual genes, we carried out "pathway analysis," which seems to be more relevant to biologic phenotypes, including therapeutic response [38]. Based on the gene expression data for ESC cell lines, we extracted a number of functionally annotated pathways whose expression was associated with the presence of *NRF2* mutation, which was also supported by ChIP-seq data of NRF2. We then used microarray data for the largest pre-CTR biopsy cohort ever reported (33 cases) and evaluated these pathways for predictive and prognostic utility. In total, up-regulation of 15 pathways was found to be significantly associated with a poor response to CRT and unfavorable prognosis, and our analysis revealed that expression of the gene sets related to oxidative stress and the immune response is associated with the clinical response of ESC to CRT and patient prognosis.

References

[1] Ferlay J, Shin HR, Bray F, Forman D, Mathers C, and Parkin DM (2010). Estimates of worldwide burden of cancer in 2008. *Int J Cancer* **127**, 2893–2917.

[2] Parkin DM, Bray F, Ferlay J, and Pisani P (2005). Global cancer statistics, 2002. *CA Cancer J Clin* **55**, 74–108.

[3] Morita M, Kumashiro R, Kubo N, Nakashima Y, Yoshida R, Yoshinaga K, Saeki H, Emi Y, Kakeji Y, Sakaguchi Y, et al. (2010). Alcohol drinking, cigarette smoking, and the development of squamous cell carcinoma of the esophagus: epidemiology, clinical findings, and prevention. *Int J Clin Oncol* **15**, 126–134.

[4] Falk GW (2009). Risk factors for esophageal cancer development. *Surg Oncol Clin N Am* **18**, 469–485.

[5] Hamilton SR and Aaltonen LA (2000). *Pathology and Genetics of Tumors of the Digestive Systems. World Health Organization Classification of Tumours*. IARC Press, Lyon, France.

[6] Kleinberg L and Forastiere AA (2007). Chemoradiation in the management of esophageal cancer. *J Clin Oncol* **25**, 4110–4117.

[7] Chirieac LR, Swisher SG, Ajani JA, Komaki RR, Correa AM, Morris JS, Roth JA, Rashid A, Hamilton SR, and Wu TT (2005). Posttherapy pathologic stage predicts survival in patients with esophageal carcinoma receiving preoperative chemoradiation. *Cancer* **103**, 1347–1355.

[8] Berger AC, Farma J, Scott WJ, Freedman G, Weiner L, Cheng JD, Wang H, and Goldberg M (2005). Complete response to neoadjuvant chemoradiotherapy in esophageal carcinoma is associated with significantly improved survival. *J Clin Oncol* **23**, 4330–4337.

[9] Martin RC, Liu Q, Wo JM, Ray MB, and Li Y (2007). Chemoprevention of carcinogenic progression to esophageal adenocarcinoma by the manganese superoxide dismutase supplementation. *Clin Cancer Res* **13**, 5176–5182.

[10] Cao L, Xu X, Cao LL, Wang RH, Coumoul X, Kim SS, and Deng CX (2007). Absence of full-length Brca1 sensitizes mice to oxidative stress and carcinogen-induced tumorigenesis in the esophagus and forestomach. *Carcinogenesis* **28**, 1401–1407.

[11] Chen X, Ding YW, Yang G, Bondoc F, Lee MJ, and Yang CS (2000). Oxidative damage in an esophageal adenocarcinoma model with rats. *Carcinogenesis* **21**, 257–263.

[12] Motohashi H and Yamamoto M (2004). Nrf2-Keap1 defines a physiologically important stress response mechanism. *Trends Mol Med* **10**, 549–557.

[13] Tong KI, Kobayashi A, Katsuoka F, and Yamamoto M (2006). Two-site substrate recognition model for the Keap1-Nrf2 system: a hinge and latch mechanism. *Biol Chem* **387**, 1311–1320.

[14] Ohta T, Iijima K, Miyamoto M, Nakahara I, Tanaka H, Ohtsuji M, Suzuki T, Kobayashi A, Yokota J, Sakiyama T, et al. (2008). Loss of Keap1 function activates Nrf2 and provides advantages for lung cancer cell growth. *Cancer Res* **68**, 1303–1309.

[15] Shibata T, Kokubu A, Gotoh M, Ojima H, Ohta T, Yamamoto M, and Hirohashi S (2008). Genetic alteration of Keap1 confers constitutive Nrf2 activation and resistance to chemotherapy in gallbladder cancer. *Gastroenterology* **135**, 1358–1368.

[16] Lee DF, Kuo HP, Liu M, Chou CK, Xia W, Du Y, Shen J, Chen CT, Huo L, Hsu MC, et al. (2009). KEAP1 E3 ligase-mediated downregulation of NF-κB signaling by targeting IKKβ. *Mol Cell* **36**, 131–140.

[17] Takahashi T, Sonobe M, Menju T, Nakayama E, Mino N, Iwakiri S, Nagai S, Sato K, Miyahara R, Okubo K, et al. (2010). Mutations in Keap1 are a potential prognostic factor in resected non–small cell lung cancer. *J Surg Oncol* **101**, 500–506.

[18] Zhang P, Singh A, Yegnasubramanian S, Esopi D, Kombairaju P, Bodas M, Wu H, Bova SG, and Biswal S (2010). Loss of Kelch-like ECH-associated protein 1 function in prostate cancer cells causes chemoresistance and radioresistance and promotes tumor growth. *Mol Cancer Ther* **9**, 336–346.

[19] Shibata T, Ohta T, Tong KI, Kokubu A, Odogawa R, Tsuta K, Asamura H, Yamamoto M, and Hirohashi S (2008). Cancer related mutations in NRF2 impair its recognition by Keap1-Cul3 E3 ligase and promote malignancy. *Proc Natl Acad Sci USA* **105**, 13568–13573.

[20] Narisawa-Saito M, Handa K, Yugawa T, Ohno S, Fujita M, and Kiyono T (2007). HPV16 E6-mediated stabilization of ErbB2 in neoplastic transformation of human cervical keratinocytes. *Oncogene* **26**, 2988–2996.

[21] Malhotra D, Portales-Casamar E, Singh A, Srivastava S, Arenillas D, Happel C, Shyr C, Wakabayashi N, Kensler TW, Wasserman WW, et al. (2010). Global mapping of binding sites for Nrf2 identifies novel targets in cell survival response through ChIP-Seq profiling and network analysis. *Nucleic Acids Res* **38**, 5718–5734.

[22] Duchesne GM (1994). Fundamental bases of combined therapy in lung cancer: cell resistance to chemotherapy and radiotherapy. *Lung Cancer* **10**(suppl 1), S67–S72.

[23] Coleman CN, Bump EA, and Kramer RA (1988). Chemical modifiers of cancer treatment. *J Clin Oncol* **6**, 709–733.

[24] Harvey CJ, Thimmulappa RK, Singh A, Blake DJ, Ling G, Wakabayashi N, Fujii J, Myers A, and Biswal S (2009). Nrf2-regulated glutathione recycling independent of biosynthesis is critical for cell survival during oxidative stress. *Free Radic Biol Med* **46**, 443–453.

[25] Ashida A, Boku N, Aoyagi K, Sato H, Tsubosa Y, Minashi K, Muto M, Ohtsu A, Ochiai A, Yoshida T, et al. (2006). Expression profiling of esophageal squamous cell carcinoma patients treated with definitive chemoradiotherapy: clinical implications. *Int J Oncol* **28**, 1345–1352.

[26] Kim YR, Oh JE, Kim MS, Kang MR, Park SW, Han JY, Eom HS, Yoo NJ, and Lee SH (2010). Oncogenic NRF2 mutations in squamous cell carcinomas of oesophagus and skin. *J Pathol* **220**, 446–451.

[27] Morita S, Yano M, Tsujinaka T, Ogawa A, Taniguchi M, Kaneko K, Shiozaki H, Doki Y, Inoue M, and Monden M (1998). Association between genetic polymorphisms of glutathione *S*-transferase P1 and *N*-acetyltransferase 2 and susceptibility to squamous-cell carcinoma of the esophagus. *Int J Cancer* **79**, 517–520.

[28] Rossini A, Rapozo DC, Soares Lima SC, Guimarães DP, Ferreira MA, Teixeira R, Kruel CD, Barros SG, Andreollo NA, Acatauassú R, et al. (2007). Polymorphisms of GSTP1 and GSTT1, but not of CYP2A6, CYP2E1 or GSTM1, modify the risk for esophageal cancer in a western population. *Carcinogenesis* **28**, 2537–2542.

[29] Zhang J, Schulz WA, Li Y, Wang R, Zotz R, Wen D, Siegel D, Ross D, Gabbert HE, and Sarbia M (2003). Association of NAD(P)H: quinone oxidoreductase 1 (NQO1) C609T polymorphism with esophageal squamous cell carcinoma in a German Caucasian and a northern Chinese population. *Carcinogenesis* **24**, 905–909.

[30] Wakabayashi N, Itoh K, Wakabayashi J, Motohashi H, Noda S, Takahashi S, Imakado S, Kotsuji T, Otsuka F, Roop DR, et al. (2003). Keap1-null mutation leads to postnatal lethality due to constitutive Nrf2 activation. *Nat Genet* **35**, 238–245.

[31] Singh A, Bodas M, Wakabayashi N, Bunz F, and Biswal S (2010). Gain of Nrf2 function in non–small-cell lung cancer cells confers radioresistance. *Antioxid Redox Signal* **13**, 1627–1637.

[32] Fareed KR, Kaye P, Soomro IN, Ilyas M, Martin S, Parsons SL, and Madhusudan S (2009). Biomarkers of response to therapy in oesophagogastric cancer. *Gut* **58**, 127–143.

[33] Höfler H, Langer R, Ott K, and Keller G (2006). Prediction of response to neoadjuvant chemotherapy in carcinomas of the upper gastrointestinal tract. *Adv Exp Med Biol* **587**, 115–120.

[34] Luthra R, Luthra MG, Izzo J, Wu TT, Lopez-Alvarez E, Malhotra U, Choi IS, Zhang L, and Ajani JA (2006). Biomarkers of response to preoperative chemoradiation in esophageal cancers. *Semin Oncol* **33**(6 suppl 11), S2–S5.

[35] Kihara C, Tsunoda T, Tanaka T, Yamana H, Furukawa Y, Ono K, Kitahara O, Zembutsu H, Yanagawa R, Hirata K, et al. (2001). Prediction of sensitivity of esophageal tumors to adjuvant chemotherapy by cDNA microarray analysis of gene-expression profiles. *Cancer Res* **61**, 6474–6479.

[36] Luthra R, Wu TT, Luthra MG, Izzo J, Lopez-Alvarez E, Zhang L, Bailey J, Lee JH, Bresalier R, Rashid A, et al. (2006). Gene expression profiling of localized esophageal carcinomas: association with pathologic response to preoperative chemoradiation. *J Clin Oncol* **24**, 259–267.

[37] Maher SG, Gillham CM, Duggan SP, Smyth PC, Miller N, Muldoon C, O'Byrne KJ, Sheils OM, Hollywood D, and Reynolds JV (2009). Gene expression analysis of diagnostic biopsies predicts pathological response to neoadjuvant chemoradiotherapy of esophageal cancer. *Ann Surg* **250**, 729–737.

[38] Murat A, Migliavacca E, Gorlia T, Lambiv WL, Shay T, Hamou MF, de Tribolet N, Regli L, Wick W, Kouwenhoven MC, et al. (2008). Stem cell–related "self-renewal" signature and high epidermal growth factor receptor expression associated with resistance to concomitant chemoradiotherapy in glioblastoma. *J Clin Oncol* **26**, 3015–3024.

Table W1. Primers and Antibodies Used in This Study.

Gene Name	Forward PCR Primer	Reverse PCR Primer	Roche Universal, No.
GCLC	ggatgatgctaatgagtctgacc	tctactctccatccaatgtctgag	25
GSR	aacaacatcccaactgtggtc	ccatatttatgaatggcttcatctt	83
GAPDH	ccaaccgcgagaagatga	ccagaggcgtacagggatag	64

Antibodies Used in This Study

Antigen	Vendor		Clone No.	Dilution for Immunoblot
NRF2	Santa Cruz	Polyclonal		×500
β-Actin	Sigma	Monoclonal	AC-15	×1000
Lamin B1	Santa Cruz	Polyclonal		×500

Table W2. Pathologic Diagnosis of the Analyzed Sarcoma Cases.

Case No.	Histology
028-L	Leiomyosarcoma
029-L	Leiomyosarcoma
032-L	Leiomyosarcoma
034-L	Leiomyosarcoma
035-L	Leiomyosarcoma
037-L	Leiomyosarcoma
038-L	Leiomyosarcoma
039-L	Leiomyosarcoma
040-L	Leiomyosarcoma
093-mL	Liposarcoma, myxoid
094-mL	Liposarcoma, myxoid
095-mL	Liposarcoma, myxoid
096-mL	Liposarcoma, myxoid
097-mL	Liposarcoma, myxoid
098-mL	Liposarcoma, myxoid
099-mL	Liposarcoma, myxoid
100-mL	Liposarcoma, myxoid
101-mL	Liposarcoma, myxoid
102-mL	Liposarcoma, myxoid
103-mL	Liposarcoma, myxoid
105-mL	Liposarcoma, myxoid
106-mL	Liposarcoma, myxoid
108-mL	Liposarcoma, myxoid
020-M	MPNST
022-M	MPNST
023-M	MPNST
024-M	MPNST
025-M	MPNST
026-M	MPNST
056-mM	Myxoid MFH
057-mM	Myxoid MFH
060-mM	Myxoid MFH
062-mM	Myxoid MFH
063-mM	Myxoid MFH
065-mM	Myxoid MFH
066-mM	Myxoid MFH
067-mM	Myxoid MFH
068-mM	Myxoid MFH
069-mM	Myxoid MFH
070-mM	Myxoid MFH
073-pM	Pleomorphic MFH
074-pM	Pleomorphic MFH
075-pM	Pleomorphic MFH
077-pM	Pleomorphic MFH
078-pM	Pleomorphic MFH
079-pM	Pleomorphic MFH

Table W2. (*continued*)

Case No.	Histology
080-pM	Pleomorphic MFH
081-pM	Pleomorphic MFH
082-pM	Pleomorphic MFH
083-pM	Pleomorphic MFH
084-pM	Pleomorphic MFH
085-pM	Pleomorphic MFH
086-pM	Pleomorphic MFH
087-pM	Pleomorphic MFH
088-pM	Pleomorphic MFH
RMS-16	Rhabdomyosarcoma
RMS-17	Rhabdomyosarcoma
RMS-18	Rhabdomyosarcoma
043-S	Synovial sarcoma
044-S	Synovial sarcoma
045-S	Synovial sarcoma
046-S	Synovial sarcoma
049-S	Synovial sarcoma
051-S	Synovial sarcoma
052-S	Synovial sarcoma
054-S	Synovial sarcoma
055-S	Synovial sarcoma
SS1	Synovial sarcoma
SS11	Synovial sarcoma
SS12	Synovial sarcoma
SS13	Synovial sarcoma
SS14	Synovial sarcoma
SS2	Synovial sarcoma
SS3	Synovial sarcoma
SS4	Synovial sarcoma
SS5	Synovial sarcoma
SS6	Synovial sarcoma
SS7	Synovial sarcoma
SS8	Synovial sarcoma
SS9	Synovial sarcoma
OS-41	Osteosarcoma
OS-44	Osteosarcoma
OS-45	Osteosarcoma
OS-46	Osteosarcoma
OS-47	Osteosarcoma
OS-49	Osteosarcoma
ES-01	Epithelioid sarcoma
ES-02	Epithelioid sarcoma
ES-04	Epithelioid sarcoma
ES-05	Epithelioid sarcoma
ES-06	Epithelioid sarcoma
ES-10	Epithelioid sarcoma

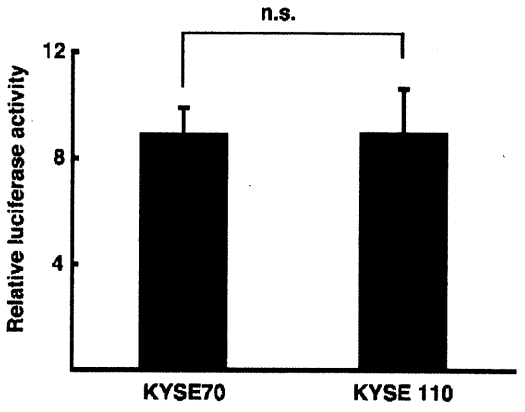

Figure W1. NRF2-dependent transcriptional activity in homozygous (KYSE70) and heterozygous (KYSE110) cells. n.s. indicates not significant.

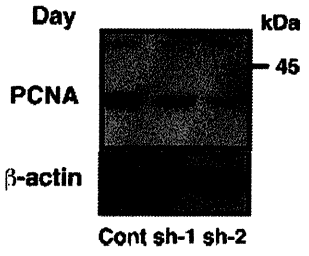

Figure W2. The expression of proliferating cell nuclear antigen (PCNA) in control (Cont) and *NRF2* (sh-1 and sh-2) shRNA expression clones. Protein extracted from each clone were immunoblotted with anti-PCNA mouse antibody (clone PC10; Cell Signaling Technologies, Danvers, MA). β-Actin was used as a loading control. Molecular marker is indicated on the right (kDa).

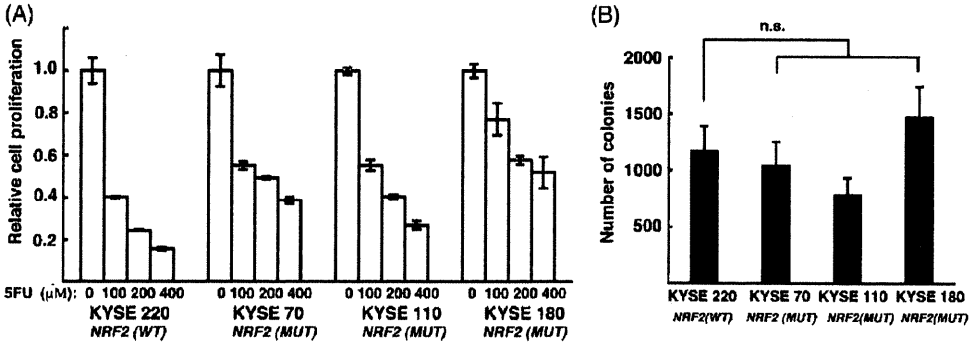

Figure W3. 5-FU sensitivity and basal colony formation capacity of *NRF2* wild-type (KYSE220) and mutated (KYSE70, KYSE110, KYSE180) ESC cell lines. (A) ESC cells were treated with various concentrations of 5-FU, and relative cell proliferation was shown. (B) Number of colony formation of each ESC cell was shown.

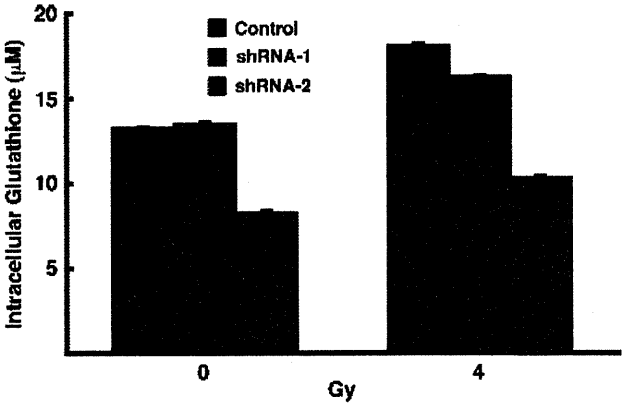

Figure W4. KYSE70 clones were irradiated (4 Gy), and the amount of intracellular reduced glutathione was measured after 24 hours.

OPEN ACCESS Freely available online

PLoS one

Artificially Induced Epithelial-Mesenchymal Transition in Surgical Subjects: Its Implications in Clinical and Basic Cancer Research

Kazuhiko Aoyagi[1], Keiko Minashi[6], Hiroyasu Igaki[3], Yuji Tachimori[3], Takao Nishimura[1], Norikazu Hokamura[3], Akio Ashida[1], Hiroyuki Daiko[4], Atsushi Ochiai[5], Manabu Muto[7], Atsushi Ohtsu[6], Teruhiko Yoshida[2], Hiroki Sasaki[1]*

1 Division of Integrative Omics and Bioinformatics, National Cancer Center Research Institute, Chuo-ku, Tokyo, Japan, **2** Division of Genetics, National Cancer Center Research Institute, Chuo-ku, Tokyo, Japan, **3** Department of Surgery, National Cancer Center Hospital, Chuo-ku, Tokyo, Japan, **4** Department of Surgery, National Cancer Center Hospital East, Kashiwa, Chiba, Japan, **5** Department of Pathology, National Cancer Center Hospital East, Kashiwa, Chiba, Japan, **6** Department of Endoscopy, National Cancer Center Hospital East, Kashiwa, Chiba, Japan, **7** Department of Gastroenterology and Hepatology, Graduate School of Medicine, Kyoto University, Sakyo-ku, Kyoto, Japan

Abstract

Background: Surgical samples have long been used as important subjects for cancer research. In accordance with an increase of neoadjuvant therapy, biopsy samples have recently become imperative for cancer transcriptome. On the other hand, both biopsy and surgical samples are available for expression profiling for predicting clinical outcome by adjuvant therapy; however, it is still unclear whether surgical sample expression profiles are useful for prediction via biopsy samples, because little has been done about comparative gene expression profiling between the two kinds of samples.

Methodology and Findings: A total of 166 samples (77 biopsy and 89 surgical) of normal and malignant lesions of the esophagus were analyzed by microarrays. Gene expression profiles were compared between biopsy and surgical samples. Artificially induced epithelial-mesenchymal transition (aiEMT) was found in the surgical samples, and also occurred in mouse esophageal epithelial cell layers under an ischemic condition. Identification of clinically significant subgroups was thought to be disrupted by the disorder of the expression profile through this aiEMT.

Conclusion and Significance: This study will evoke the fundamental misinterpretation including underestimation of the prognostic evaluation power of markers by overestimation of EMT in past cancer research, and will furnish some advice for the near future as follows: 1) Understanding how long the tissues were under an ischemic condition. 2) Prevalence of biopsy samples for *in vivo* expression profiling with low biases on basic and clinical research. 3) Checking cancer cell contents and normal- or necrotic-tissue contamination in biopsy samples for prevalence.

Citation: Aoyagi K, Minashi K, Igaki H, Tachimori Y, Nishimura T, et al. (2011) Artificially Induced Epithelial-Mesenchymal Transition in Surgical Subjects: Its Implications in Clinical and Basic Cancer Research. PLoS ONE 6(4): e18196. doi:10.1371/journal.pone.0018196

Editor: Irene Oi Lin Ng, The University of Hong Kong, Hong Kong

Received December 24, 2010; **Accepted** February 22, 2011; **Published** April 21, 2011

Funding: This study was supported in part by the Program for Promotion of Fundamental Studies in Health Sciences of the National Institute of Biomedical Innovation; a Grant-in-Aid for the Third Comprehensive 10-Year Strategy for Cancer Control from the Ministry of Health, Labour and Welfare of Japan; Princess Takamatsu Cancer Research Fund, and Foundation for Promotion of Cancer Research (RR: T.N.). The funders had no role in study design, data collection and analysis, decision to publish, or preparation of the manuscript. No additional external funding received for this study.

Competing Interests: The authors have declared that no competing interests exist.

* E-mail: hksasaki@ncc.go.jp

Introduction

Cancer is a major cause of human deaths in many countries. Gene expression profiles from DNA microarrays are individualized and useful in the diagnosis and prognosis of diseases [1]. Although some artificial factors such as ischemia, hypoxia, hyponutrition, and cold stress possibly occur during surgical resection and sample transportation (Figure S1), surgical samples have long been used as important subjects for clinical and basic cancer research. In accordance with an increase of neoadjuvant therapy (in head and neck, esophageal, lung, pancreatic, prostate, and breast cancers), biopsy samples have recently become imperative for cancer transcriptome. On the other hand, both biopsy and surgical samples are available for expression profiling for predicting clinical outcome by adjuvant therapy (in stomach, colon, liver, bladder, pancreatic, brain, kidney, ovarian, cervical, and breast cancers). The targets for microarray analysis were, for the last ten years, mostly surgical samplesfrom the development and prevalence of two types of microarray: oligonucleotide [2, 3] and cDNA [4, 5]. However, whether a huge number of accumulated surgical sample expression profiles are useful for prediction by the use of biopsy samples from pretreated patients is still unclear, because little has been done about comparative gene expression profiling between the two kinds of samples.

Chemoradiotherapy (CRT) followed by surgery is the standard therapy for esophageal cancer in Western countries. In Japan,

neoadjuvant chemotherapy followed by surgery and definitive CRT are the standard therapies [6], and for locally advanced esophageal cancers (Stage II or III), surgery was the standard therapy there approximately 5 years ago [7]. This enables us to obtain both biopsy and surgical samples from esophageal cancer patients and to compare gene expression profiles between these two kinds of samples. Here we report that artificially induced epithelial-mesenchymal transition (aiEMT) occurs in surgical samples. Its presence there has possibly interfered not only with microarray- or immunohistochemistory-based clinical research but also with basic research.

Results

Comparison of Expression Profiles between Biopsy and Surgically Resected Esophageal Tumor Samples Obtained from Different Cases

We first compared gene expression profiles between 35 fresh biopsy samples containing no necrotic lesion and 66 surgical esophageal tumor samples, which were obtained from a margin of the tumor after exposure for 4–7 hours under an ischemic condition, by unsupervised clustering with 3,126 processed genes (Materials and Methods). There was no significant difference in clinical or pathological stage distribution between these two sets of esophageal cancers because locally advanced tumors (Stage II or III) are major targets of both chemoradiotherapy and surgery [8–10]. Sixty of the 66 surgical samples (90.9%) and 29 of the 35 biopsy samples (82.9%) appeared in a (left) and b (right) sample cluster, respectively (Figure 1A). To investigate the number of differentially expressed genes between these two kinds of samples with reproducibility, we compared expression profiles among three independent sample sets (A, B, and C): another 20 biopsy sample set versus three surgical sample sets (A, B, and C) containing 20 randomly selected cases from the 66 cases (Figure 1B, upper). The number of differentially expressed genes selected by u-test ($p<0.01$) were 2, 295, 2,328, and 2, 245 in sets A, B, and C, respectively. Among these 3 sets, 1,495 genes (65.1% in A, 64.2% in B, and 66.6% in C) were commonly identified (Figure 1B, upper). Therefore, more than 20% (1,495/6,000, 24.9%) of the genes were differentially expressed between biopsy and surgical samples because the average number of detectable genes in each case was approximately 6,000. These results suggested that a large difference exists between the biopsy and surgical samples.

From the 1,495 genes, we further selected differentially expressed genes among the 3 sets that had a 3-fold change between two average signal intensities of each gene between the biopsy and surgical samples. From sets A, B, and C, 297, 273, and 300 genes were identified, respectively (Figure 1B, lower). More than 80% of these genes were over-expressed in the surgical samples, suggesting a preferential presence of artificial factors or a contamination of normal portions.

To address the rationale for the difference, we finally selected genes that expressed preferentially in all the 35 biopsy or 66 surgical samples under stringent conditions with u-test ($p<0.01$), permutation test, and a 2-fold change, etc. (Materials and Methods). By this procedure, 38 and 219 genes were identified as up-regulated genes in the biopsy and surgical samples, respectively (Table S1 and Figure 1C). Interestingly, in the surgical samples, many EMT markers were found to be expressed preferentially and frequently. Microarray results of 13 representative EMT markers including fibronectin (FN), vimentin (VIM) and collagens (COLs) are shown in Figure 2A. Moreover, membrane signal transducers such as cytokine, chemokine, and receptors were also found to be up-regulated in the surgical samples. Representative microarray and RT-PCR results of *IL8*, *CXCR4*, *CXCL9*, *PDGFRB*, *CCL5*, and *TLR2*, respectively are shown in Figures 2B and 2C. In correspondence with EMT, E-cadherin (*CDH1*) was found to be down-regulated in the surgical samples (Figure 2A, right lowest).

Comparison of Expression Profiles between Biopsy Samples and Surgical Resected Esophageal Tumor Samples Obtained from Identical Cases

In the same above way, we compared gene expression profiles between 18 biopsy and 18 surgically resected esophageal tumor samples, and selected 41 and 716 genes that were identified as up-regulated genes in the two kinds of samples, respectively (Table S2 and Figure 3). In accordance with the above results from different cases, many EMT markers and membrane signal transducers were also found to be up-regulated frequently in the surgical samples (Figure 4A). More importantly, two EMT regulators, *ZEB1* and *ZEB2*, and some EMT-related myogenic transcription factors including *MEOX2* and *MEF2C* were able to be selected as up-regulated genes in the surgical samples (Figures 4A). Quantitative real-time RT-PCR confirmed over-expression of *ZEB1*, *ZEB2*, *FN*, *and VIM* in the 18 surgical samples of identical cases (Figure 4B). The over-expression of *ZEB1* and *ZEB2* was also found in the 66 surgical samples of different cases (Figure S2), although these two EMT regulators could not be extracted from expression profiles under the above stringent conditions. SNAI1/Snail, SNAI2/Slug, ZEB1/ZFHX1A, ZEB2/SIP1/ZFHX1B, TWIST1/TWIST, and TWIST2 are representative EMT regulators [11, 12]. Among them, *TWIST1* as well as two *ZEBs* were over-expressed in the two sets of esophageal tumors (Figure S3). To investigate whether aiEMT in the mRNA levels affects immunohistochemistry (IHC), we performed IHC on a typical mesenchymal marker vimentin in biopsy and surgical samples of identical cases. First we determined conditions under which normal epithelial cell layers could not be stained, but tumor cells with EMT could be (Figures 5A, 5B), because undifferentiated layers (basal and parabasal) have been reported to express EMT-related genes including *VIM* [4]. In 3 out of 5 pairs of the samples examined, tumor lesions of a surgical sample were found to be stained more highly than those of a biopsy sample (Figures 5C–H); however, the remaining 2 pairs did not show such difference (data not shown). Therefore, the aiEMT that occurred in the surgical samples in the mRNA level was thought to affect only a subset of surgical samples in the level of EMT-related proteins.

Over-expression of *ZEB1*, *ZEB2*, and *TWIST1* in Surgically Resected Normal Tissues

We obtained 4 biopsy samples and 5 surgical samples of non-cancerous tissues, and compared their expression profiles. In the same manner with the above expression profiles of tumor tissues (Figures 2, 4, S2, and S3), three EMT regulators (*ZEB1*, *ZEB2*, and *TWIST1*) and two typical EMT markers (*VIM* and *FN*) were found to be over-expressed in the 5 surgical samples (Figure 6A). Our previous report showing the involvement of ZEB2 and TWIST1 in the EMT of normal and malignant esophageal epithelial cells [9] supports the presence there of artificially induced EMT.

Finally, to investigate whether these 5 genes are induced in epithelial cells by surgical resection-related ischemia, we resected a mouse esophagus, and placed it on PBS for 0 or 4 hours, and immediately made frozen sections followed by laser-captured microdissection of the epithelial cell layers (Figure 6B, upper). Expression profiles of the mouse epithelial cell layers at 0 or

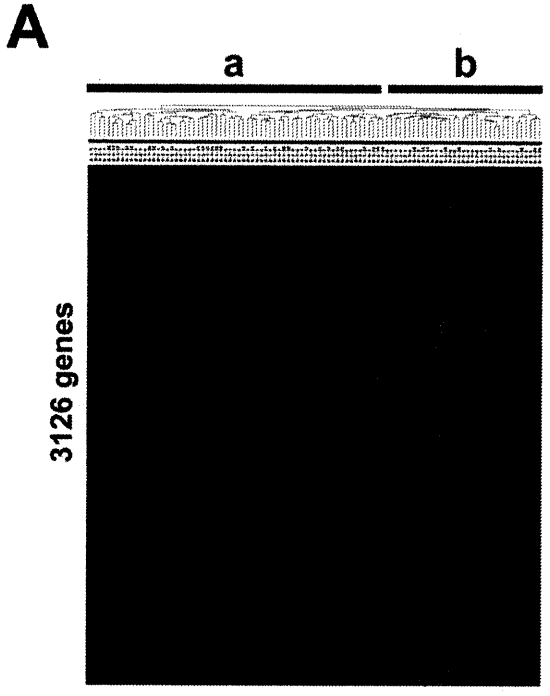

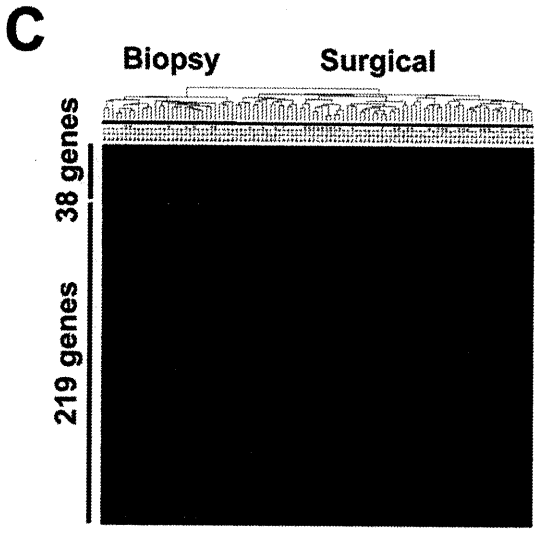

B

	Comparison	1. > 1000 signal intensity in > 10% sample 2. u-test ($p < 0.01$)
Set A	20 biopsy vs. 20 surgical A	2295
Set B	20 biopsy vs. 20 surgical B	2328
Set C	20 biopsy vs. 20 surgical C	2245

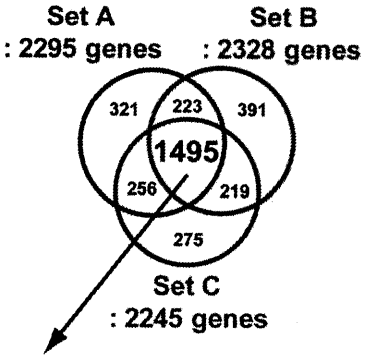

> 3 fold change between average signal intensities of surgical and biopsy samples

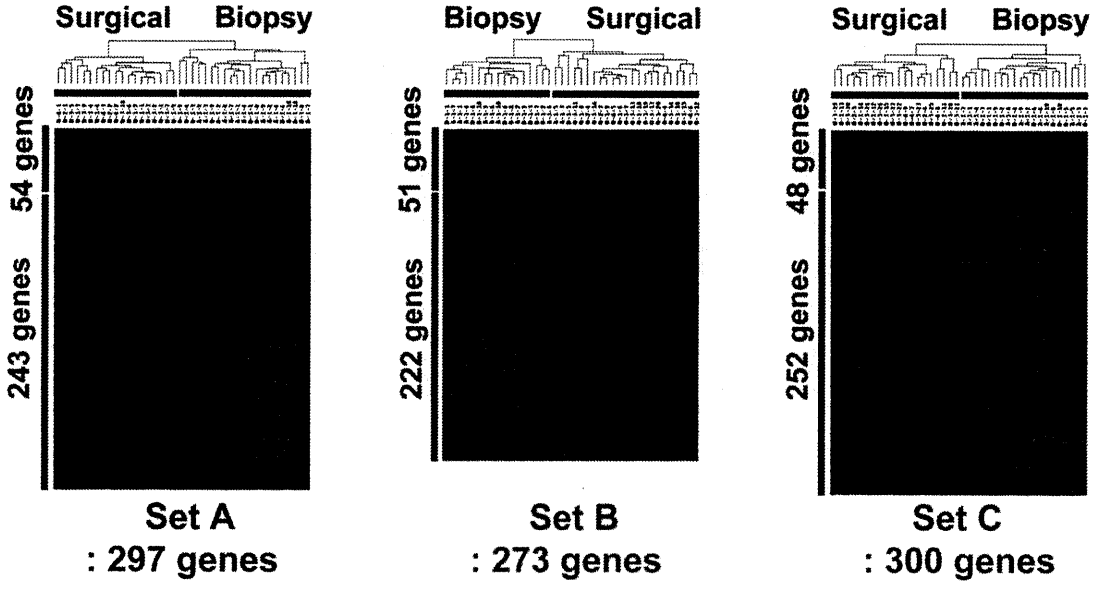

Figure 1. Comparison of expression profiles between biopsy and surgically resected esophageal tumor samples obtained from different cases. (A) Unsupervised clustering with 3,126 processed genes. Surgical (a) and biopsy sample clusters (b) are shown. (B) Comparison of expression profiles among three independent sets (A, B, and C): a randomly selected 20-biopsy sample set versus three surgical sample sets (A, B, and C) containing 20 independent cases. The number of differentially expressed genes selected by u-test ($p<0.01$): 2, 295 in set A, 2,328 in set B, and 2, 245 in set C (Upper). The number of differentially expressed genes with a 3-fold change between two average signal intensities: 297, 273, and 300. Clustering results with these gene sets (Lower). (C) Up-regulated genes in surgical or biopsy samples. By the use of all of the profiles under stringent selection conditions (see Materials and Methods), 38 and 219 genes were identified as up-regulated genes in the biopsy and surgical samples, respectively.
doi:10.1371/journal.pone.0018196.g001

4 hours after resection revealed that mouse *Zeb1*, *Zeb2*, *Vim*, and *Fn* were induced 4 hours after resection (Figure 6B, lower). Quantitative real-time RT-PCR confirmed over-expression of *Zeb1*, *Zeb2*, *Vim*, and *Fn* after resection (Figure 6C). Since overall sensitivity of mouse affymetrix arrays is known to be lower than in humans, and the use of a small amount of RNA such as laser-captured subjects is also known to reduce microarray sensitivity, *Twist1* mRNA itself could not be detected in this mouse experiment (data not shown).

To investigate whether aiEMT in the mRNA levels affects IHC, we performed IHC on a typical mesenchymal marker vimentin 8 hours after resection. Here we determined conditions under which normal epithelial cell layers are stained. In all of the 3 independent samples examined, normal epithelial cell layers were not found to be stained highly 8 hours after resection (Figures 7A–C). The discrepancy between the mRNA level and protein level can be explained by the two following reasons: 1) although undifferentiated layers (basal and parabasal) have been reported to express EMT-related genes including *VIM* [4], their expression levels were much lower than tumor (Figure 5B). 2) it may also be difficult to show the approximate 2-fold change in the mRNA level (Figures 6B, C) as in the protein level by IHC, because IHC is inferior to RT-PCR in both sensitivity and quantification.

All of the results suggest that EMT, especially in the mRNA level, is induced artificially in both normal and malignant epithelial cells by surgical resection-related events (ischemia-induced hypoxia and hyponutrition, and hypoxia-induced inflammation, etc.).

Artificially Induced EMT (aiEMT) by Surgical Resection Prevents Microarray-based Subgroup Identification

Identification of clinically significant subgroups is very important for personalized medicine and for drug development against intractable cases. When we used the expression profiles of the 35 biopsy samples obtained from patients treated by chemoradiotherapy [8], unsupervised clustering with 5,570 processed genes (Materials and Methods) identified a good responder group consisting of 9 patients (7/9, 78% showing complete response to chemoradiotherapy) from the 35 (Figure 8A, left). However, when the profiles of the 66 surgical samples were used, unsupervised clustering with 2,016 processed genes could not identify any subgroup (Figure 8A, right). Thus, biopsy sample expression profiles seemed to be more effective in subgroup identification than those of the surgical samples. In fact, we previously reported that biopsy sample expression profiles could distinguish long-term or short-term survivors by definitive chemoradiotherapy [8]; however, surgical sample expression profiles never identified poor prognostic subgroups with extensive lymph node metastasis [10]. Moreover, in the surgical samples, EMT was accelerated in 36 (85.7%) out of 42 esophageal cancers [9]. This high percentage seems to be caused by aiEMT.

To address the reason why subgrouping is difficult in surgical samples, we compared the number and distribution of each of the processed genes, which were used for unsupervised clustering. We first selected genes with a signal intensity of more than 1,000 in more than 10% of the samples. From 35 biopsy and 66 surgical samples, 6,551 and 4,797 genes, respectively, were selected. From these genes, we finally selected more than 3-fold changed genes by comparing the average signal intensity of each gene in more than 10% of the samples. In the 35 biopsy samples, 85% (5,570) of 6,551 first processed genes remained, whereas the number of final processed genes decreased from 4,797 first processed genes to 2,016 (42%) (Figure 8B, upper). Of the 2,016 finally processed genes in the surgical samples, 1,724 (86%) were included in the 5,570 finally processed genes in the biopsy samples; however, 3,846 (69%) of 5,570 genes were unique to the biopsy samples (Figure 8B, lower). Moreover, frequency distribution (for percentage of samples) of these two finally processed-gene sets shows that approximately 60% of the 2,016 processed genes in the surgical samples express in only a limited number of cases (0–10%) (Figure 8C). Accordingly, aiEMT in surgical samples may diminish the number of processed genes useful for subgroup identification.

Discussion

We recently reported the presence of crosstalk between Hedgehog (Hh) and EMT signaling in normal and malignant epithelial cells of the esophagus [9]. In that report, *ZEB2* was shown to be a downstream gene of both a primary transcriptional transducer GLI1 in Hh signaling and of another EMT regulator, TWIST1, and that ZEB2 further up-regulated 5 chemokine or growth factor receptors, *PDGFRA*, *EDNRA*, *CXCR4*, *VEGFR2*, and *TRKB* (Figure S4). The Hh signal block inhibited esophageal keratinocyte differentiation and cancer cell invasion and growth. Accordingly, over-expression of *ZEB2* and *TWIST1* in surgical samples of both normal and tumor tissues can induce EMT, resulting in over-expression of representative EMT markers *VIM*, *FN*, and *COLs* (Figures 2, 4, 6, S2, and S3) and membrane signal transducers *IL8*, *CXCL4*, *CCL5*, *CXCR4*, *PDGFRB*, and *TLR2* (Figure 2). Over-expression of the membrane signal transducers can activate further down-stream cascades. This is a major reason for the large difference of expression profiles between biopsy and surgical samples (Figures 1 and 3).

Extensive contamination of normal mesenchymal portions in surgically resected tumor tissues can also explain the over-expression of those EMT regulators and EMT-related genes, even though trained pathologists carefully excised bulk tissue samples from the main tumor, leaving a clear margin from the surrounding normal tissue (Materials and Methods). However, the over-expression was also observed in surgically resected normal tissue and mouse epithelial cell layers 4 hours after resection (Figure 6). Therefore, we concluded that artificially induced EMT, termed aiEMT, occurred in both normal and malignant epithelial cells by the surgical resection-related events (ischemia-induced hypoxia, ischemia-induced hyponutrition, and hypoxia-induced inflammation, etc.) (Figure S1).

Recently, the hypoxia-inducible factors (HIF-1A or HIF-2A) have been reported to directly regulate TWIST1 [13, 14] and

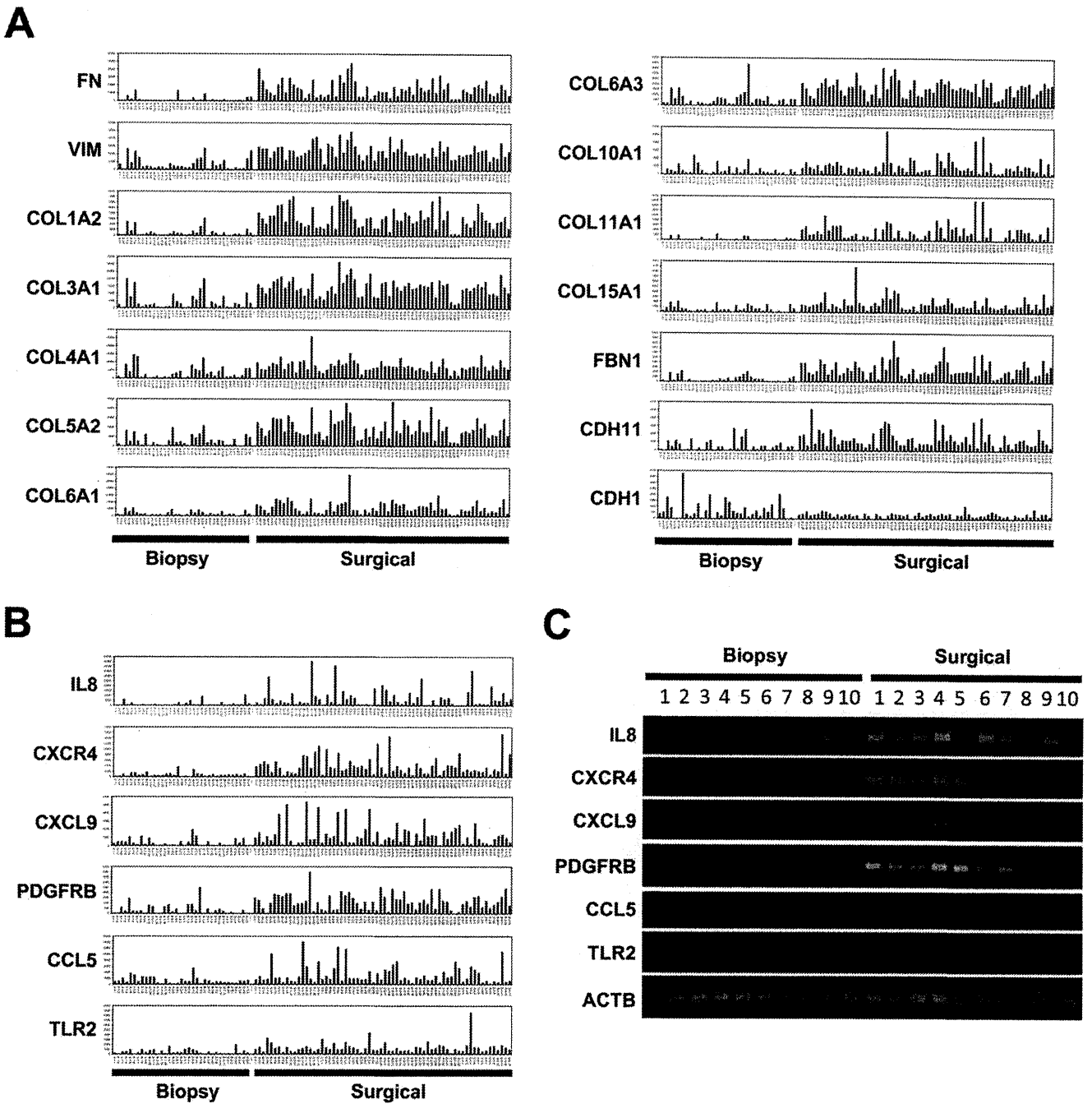

Figure 2. Representative EMT related genes over-expressed in surgically resected esophageal tumor samples. (A) Expression patterns of an epithelial cell marker E-cadherin (*CDH1*) and typical EMT markers including fibronectin (*FN*), vimentin (*VIM*), and collagens (*COLs*). (B) Expression patterns of 6 membrane signal transducers: a cytokine (*IL8*), two chemokines (*CXCL9* and *CCL5*), and three membrane type receptors (*CXCR4*, *PDGFRB*, and *TLR2*). (C) Semi-quantitative RT-PCR results of these 6 membrane transducers in representative samples.
doi:10.1371/journal.pone.0018196.g002

LOXL2, which reportedly stabilized an EMT regulator, SNAI1/SNAIL, through physical interaction on the SLUG domain and Snail's lysine residues K98 and K137 [15]. The SNAI1 binding site was also found in the 5' promoter region of *ZEB2* [16]. Over-expression of both *HIF1A* and *LOXL2* was observed only in the surgically resected tumor tissues obtained from different cases (Figure S5). Moreover, other *HIF1* families (*HIF1B* and *HIF2A*) were never over-expressed in any of the surgical samples. Therefore, elucidation of the molecular mechanisms of aiEMT in surgical samples remains for future studies. However, we noted that ischemia-induced hypoxia and/or inflammation has been reported to release repression of NFκB [17], which regulates *ZEB1*, *ZEB2*, and *TWIST1* [18, 19] and that TGF-β signaling may be involved in aiEMT, because over-expression of *NFKB1* and *TGFBR2* was found in surgical samples (Figure S6).

As mentioned in the Introduction, surgical samples have been used as important subjects for clinical and basic cancer research for many years. Therefore, aiEMT in surgical samples may have possibly interfered with or prevented not only microarray- or immunohistochemistry-based clinical research (diagnostic marker

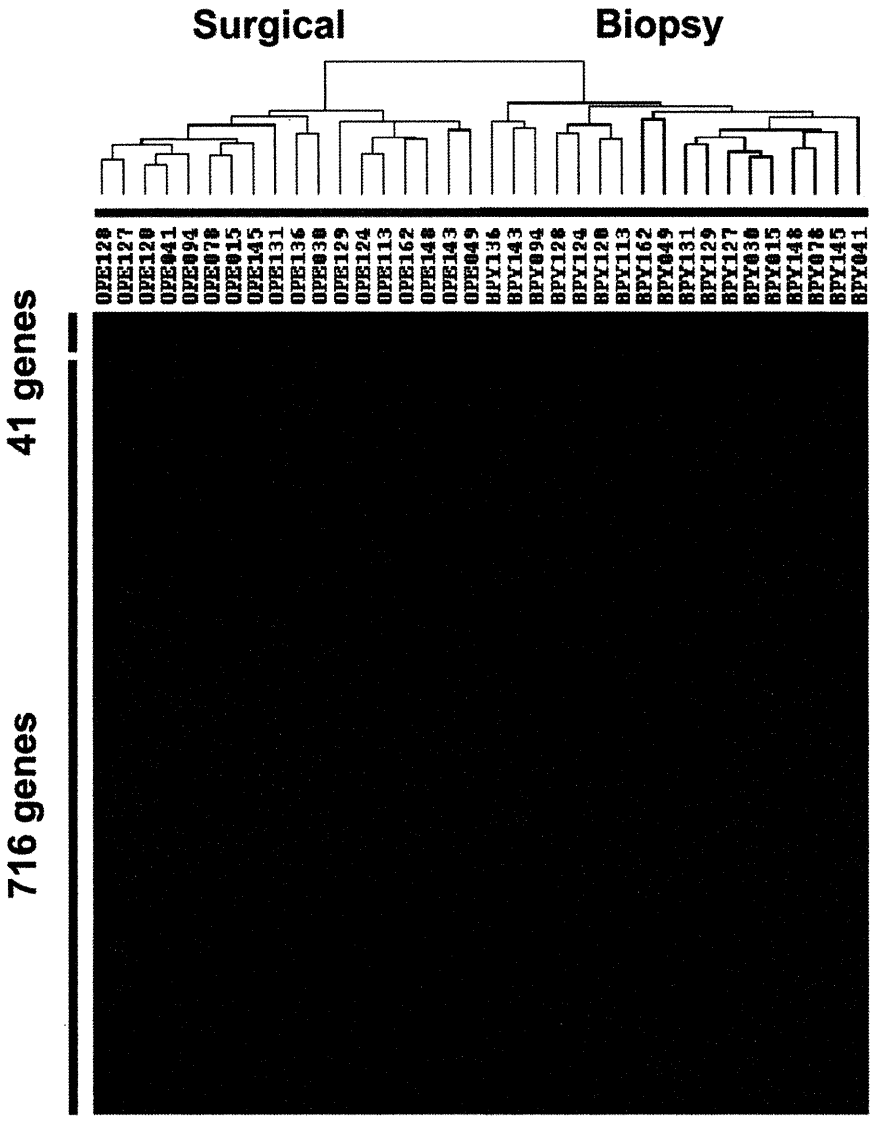

Figure 3. Up-regulated genes in biopsy and surgically resected esophageal tumor samples obtained from identical cases. By stringent selection (see Materials and Methods), 41 and 716 genes were identified as up-regulated genes in the biopsy and surgical samples, respectively.
doi:10.1371/journal.pone.0018196.g003

identification, subgrouping, making predictors, and prognosis evaluation, etc.) but also basic research (making a signal pathway map, therapeutic target identification, etc.). This study will likely evoke fundamental misinterpretation including underestimation of the prognostic evaluation power of markers by overestimation of EMT in past cancer research, and will provide some advice for the near future as follows: 1) Understanding how long the tissues were under an ischemic condition (from start of resection to stock or RNA preparation). The total amount of time should never exceed 4 hours. 2) Prevalence of biopsy samples for *in vivo* expression profiling with low biases on basic and clinical research; for example, for clinical outcome prediction of not only neoadjuvant but also adjuvant chemotherapy, radiotherapy, and chemoradiotherapy such as in previous reports [8, 20–23]. 3) Checking cancer cell contents and normal- or necrotic-tissue contamination in biopsy samples for the prevalence. In sampling by a needle biopsy, tumor portions (2mm X 2mm) should be obtained from a margin (periphery) of the tumor by exclusion of central necrotic lesions under endoscopy. If necrotic lesions were severely contaminated in the samples, those samples should be excluded by quantifying and qualifying RNA. If the samples contained extensive normal lesions, such samples can be excluded by the expression profile-based scoring method using normal and/or tumor specific genes.

Materials and Methods

Tissue Samples

All esophageal cancer (squamous cell carcinomas) and non-cancerous tissues were provided by the Central Hospital or East Hospital at the National Cancer Center after obtaining written informed consent from each patient and approval by the Center's Ethics Committee.

All surgical samples were obtained from patients without neoadjuvant therapy, and all biopsy samples were obtained before treatment. For the surgical samples, trained pathologists carefully excised bulk tissue samples from the main tumor, leaving a clear

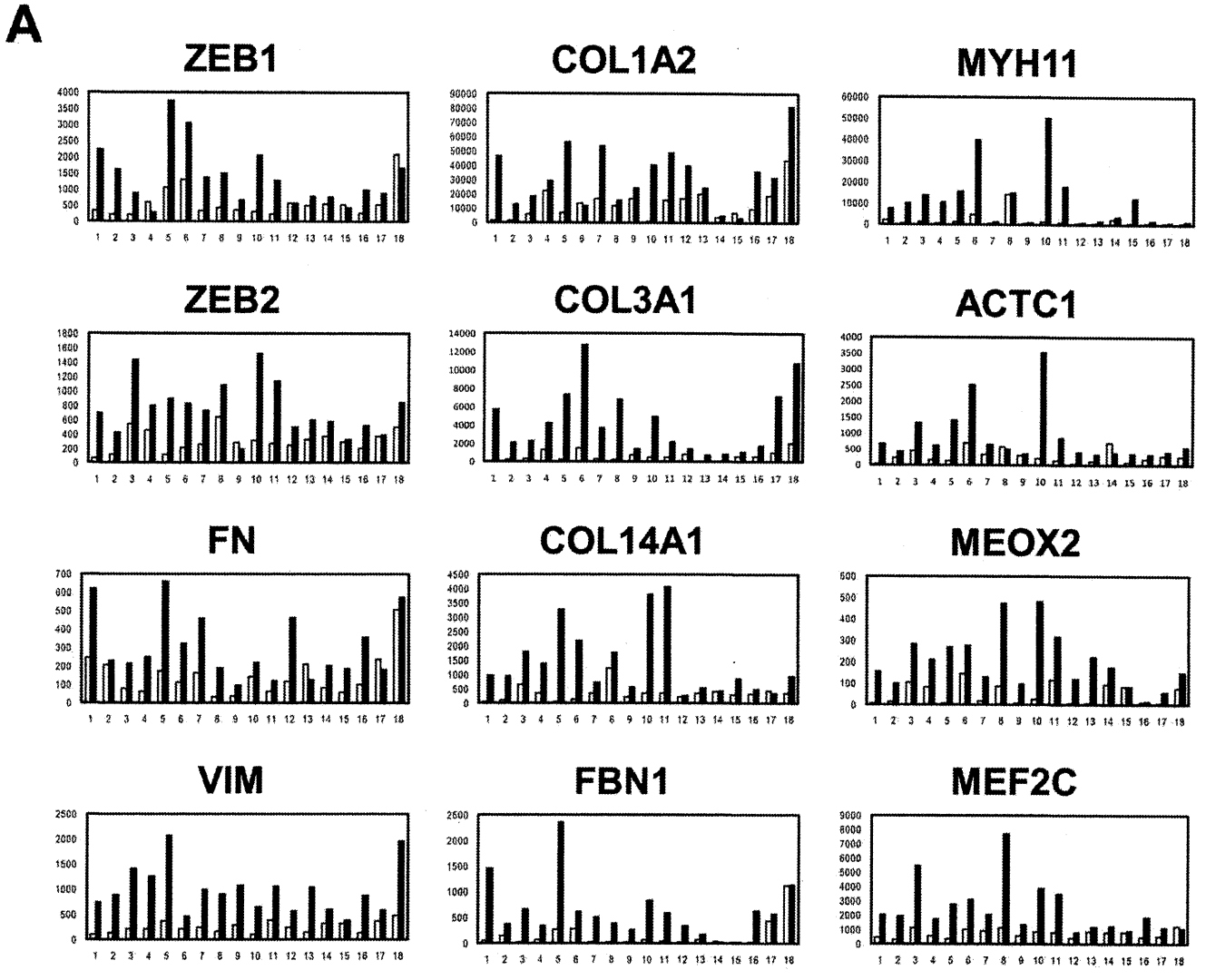
A
ZEB1
COL1A2
MYH11
ZEB2
COL3A1
ACTC1
FN
COL14A1
MEOX2
VIM
FBN1
MEF2C

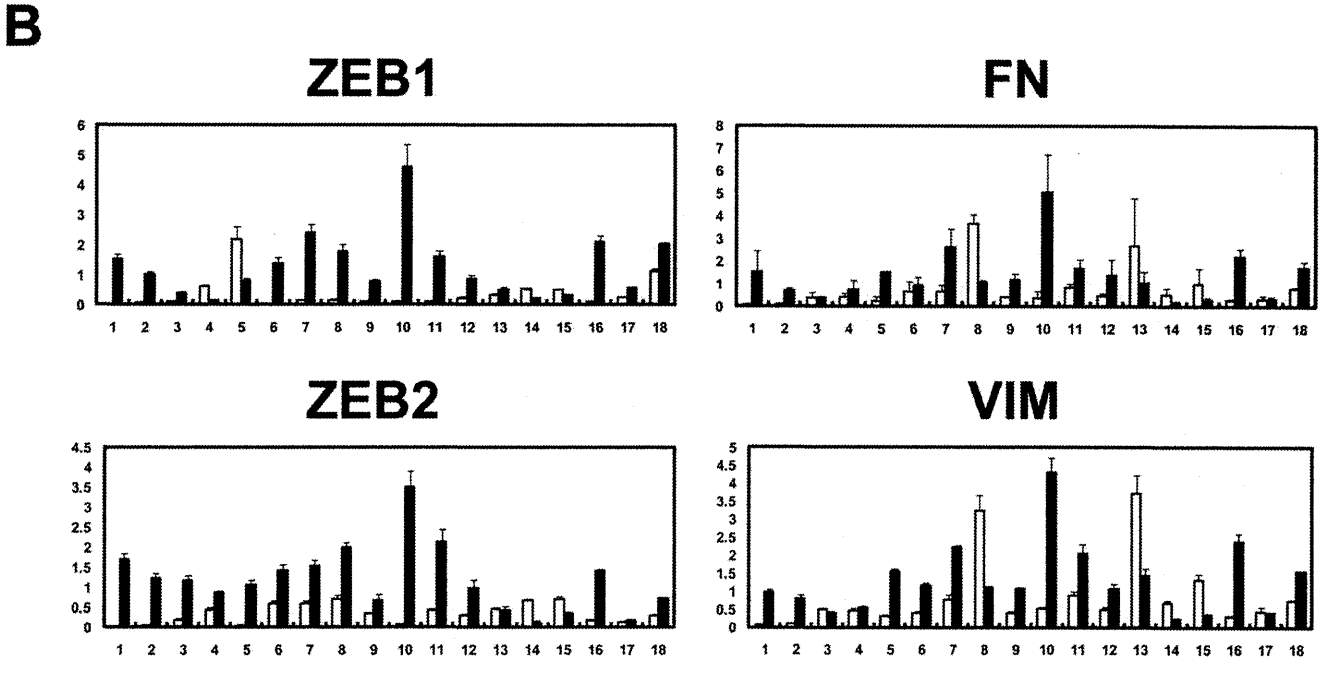
B
ZEB1
FN
ZEB2
VIM